THE UNITED NATIONS UNIVERSITY

ORKUSTOFNUN
NATIONAL ENERGY AUTHORITY

DELIVERABILITY OF GEOTHERMAL RESERVOIRS

Jesús de León Vivar

Geothermal Training Programme
Reykjavík, Iceland
Report 2, 1988

Report 2, 1988

DELIVERABILITY OF GEOTHERMAL RESERVOIRS

Jesús de León Vivar
UNU Geothermal Training Programe
National Energy Authority
Grensásvegur 9
108 Reykjavík
ICELAND

Permanent Address:
Gerencia de Proyectos Geotermoélctricos
Comisión Federal de Electicidad
Alejandro Volta 655
Col.Electricistas
Morelia, Mich.
MEXICO

ABSTRACT

Deliverability of a geothermal field is divided in to wellbore performance, inflow performance and reservoir performance. Wellbore performance curves for in the Svartsengi geothermal field in Iceland were estimated at different wellhead pressures using a two-phase flow wellbore simulator. Inflow performance curves were estimated using linear, turbulent and two-phase equations and compared with data for in the Cerro Prieto geothermal field in México. Reservoir performance of the Svartsengi field was calculated using Hurst radial water influx models. The three performances were linked in a sample calculation to determine the deliverability typical for the Svartsengi field.

LIST OF CONTENTS

TABLES

FIGURES

INTRODUCTION

The optimization of geothermal energy production is a task of the reservoir engineer. For this purpose it is necessary to know how the different parts of the overall system intervene in the production of steam. The concept of deliverability help to explain part of that. The deliverability of a geothermal reservoir can be divided into three components: wellbore performance, inflow performance and reservoir performance.

Wellbore performance is the contribution of casing for transporting the fluid from the bottom to the top in the well when there is a pressure drop. Other hand, the inflow performance is strong function that describes the ability of geothermal fluid to flow through the feedzone when there is a pressure drop between the reservoir and the well bottom. The fluid can present laminar, turbulent, two-phase effects or combination of these. The reservoir performance is a dynamics variable that says how the reservoir pressure has been changing with the time.

These components have been studied in this work. Data from Svartsengi geothermal field in Iceland and Cerro Prieto geothermal field in México have been used to show the methodology for working with these conceptions.

WELLBORE PERFORMANCE

Wellbore performance describes fluid pressure behavior in the casing and liner between the bottom or the main feed zone to the well head (Marcou, 1985). This performance depends on different variables, including: fluid temperature and pressure, well diameter and depth (Marcou and Gudmundsson, 1986). In the geothermal it industry is common test a well at different wellhead pressures to know what will be its capacity of this. The flow enters the wellbore and travels

through the casing. It depends on the restriction (diameter of orifice or valve) at the well head and the variables mentioned before, it will produce certain mass and well head pressure. Wellbore performance was calculated at different wellhead pressures in this work. Thermodynamic fluid conditions determine the phase of the fluid; It can be one or two-phase.

Wellbore performance can be represented by curves that related the well flowing pressure to the mass flowrate at the main feed zone of the well. Flowing pressures at depth are difficult to measure in geothermal wells due to high mass flowrate. Therefore single or two-phase wellbore simulator must be used to calculate wellbore performance. A state-of-the-art wellbore simulator was employed is this work (Ortiz, 1983).

The casing size is the only factor that can be optimize in wellbore performance. Figure 1 shows two different curves for 9-5/8 in. and 13-3/8 in. sizes of casing, (Marcou and Gudmundsson, 1986). They indicate that as the well flowing pressure increases, the mass flow rate increases. The 13-3/8 casing presents lower pressure drop and more mass flow than 9-5/8 in. casing.

Wellbore performance curves were calculated for five wells in the Svartsengi geothermal field. Wells 7, 8, 9, 11 and 12 are 1436 m, 1609 m, 994 m, 1141 m and 1488 m deep respectively. All of them have a 13-3/8 in. casing. Well 12 has this type of casing to 607 m and is barefoot 12-1/4 in. to bottom. The wellbore performance was calculated at the main feedzone of each well, determined from a figure (Figure 1) in Gudmundsson and Olsen (1987). They are shown in Table 1 with the well casing depth. The same reservoir temperature 238°C, and enthalpy, 1028 kJ/kg, for wells 7, 8, 9 and 11, were used. They were determined by Bjarnason (1988). Well 12 however has a reservoir temperature of 220-235°C and an enthalpy of 1000 kJ/kg (Gudmundsson, 1984).

The wellbore performance curves were calculated for each well to different mass flowrates. These were selected between 60 and 120 kg/s; that is above and below the data reported by Gudmundsson and Olsen (1987). The well head pressure was varied between 0.5 and 1.2 MPa. The flowing pressures were determined using the wellbore simulator of Ortiz (1983), with the conditions of reservoir temperature, enthalpy, casing diameter, mass flowrate and well head pressure mentioned before. One example of output data results of the wellbore simulator from well 7 are shown in Appendix A.

Flowing pressure results of the wells 7, 8, 9 and 12 of Svartsengi geothermal field are given in the Tables 2, 3, 4 and 5. The wellbore performance curves were graphed with the data from these tables and are shown in the Figures 2 to 5.

Two different behaviors can be observed above and below the saturation pressure in these graphs. Above saturation pressure the curves tend to bend upward to the vertical and according to Marcou (1985), this indicates the limit of flow capable of carried by the pipe for the given conditions. One example is the wellbore performance of the well 12, Figure 4.

When flowing pressure are below the saturation pressure the wellbore performance curves are smooth, almost a straight line. All the curves might be joint in one straight line if the substraction is obtained between flowing pressure and wellhead pressure and after to take the square root. Two examples of these are wells 7 and 9 (well 11 too, because it has the same conditions of the well 9) where its flowing pressure are below of saturation pressure, Figure 2 and 4. The curves are jointed in one straight line with the procedure mentioned before. These are shown in Figure 6 and 7. Two-phase well can be defined with this procedure and by example any bottom flowing pressure could be rapidly determined if mass flowrate and wellhead pressure are known.

Well 8 does not present this characteristic, if the square root of the substraction of its pressures is obtained the graph does not present a good fit, Figures 8. It is due to that the flowing pressure data are above and below on saturation pressure.

The main advantage of expressing the wellbore performance in graphical form in that it can easily be combined with inflow performance curves to predict field deliverability (Marcou, 1985).

INFLOW PERFORMANCE

Inflow performance describes the ability of geothermal fluid to flow through the feedzone when there is a pressure drop between the reservoir and the well bottom. The reservoir pressure provides the driving force to move fluid to the well. The inflow performance depends on the different variables including: reservoir pressure, well bottom flowing pressure, permeability, formation thickness, fluid properties, drainage radius and formation skin.

Laminar Flow

In the oil industry it is commonly assumed that inflow into a well is directly proportional to the pressure difference between the reservoir and weellbore and that production is directly proportional to drawdown. The constant of proportionality is the productivity index, P.I. derived from Darcy's law, (Vogel, 1968). This concept has been used by Gudmundsson (1984), for calculating output curves of geothermal wells with single phase feedzone using a wellbore simulator. The equation that define the productivity index for single phase laminar flow is

$$\frac{\Delta w}{\Delta w_{max}} = 1.0 - 0.2\,[p_{wf}/p_{sat}] - 0.8\,[p_{wf}/p_{sat}]^2 \qquad (4)$$

The Δw is the incremental mass flowrate achieved by lowering the well flowing pressure below the fluid's saturation pressure. The Δw_{max} is would ideally be achieved if the well flowing pressure became negligible. In other words, if there was negligible pressure drop in the wellbore. The square term in the modified Vogel relationship takes into account turbulent losses and other non-linear effects (Marcou and Gudmundsson, 1986). The problem in the Equation 4 is to know Δw_{max}. Equation 5 was derived here to find Δw_{max} and is the develop as presented in Appendix B.

$$\Delta w_{max} = -\frac{p_{sat}}{1.8}\left(\frac{1}{dp/dw}\right) \qquad (5)$$

Pseudosteady-State Solution

Three transient flow regimes might be expected in a reservoir: infinite, transition and pseudosteady-state (Erlougher, 1977). These are shown in Figure 9. When the last one of these is reached or when the pressure change with time dp/dt is constant at all points in the reservoir, the pseudosteady-state solution equation for a large-time can be utilized to estimate the productivity index of a well.

Suppose a well producing at the center of a circular, liquid dominated, homogeneous medium with a thickness h reservoir in pseudosteady-steady period, the solution of the diffusivity equation for this conditions takes the form:

$$p_r - p_{wf} = \frac{w\mu\nu}{2\pi kh}\,(\ln r_r/r_w) \qquad (6)$$

the productivity index might be obtained

$$P.I. = \frac{w}{p_r - p_{wf}} \qquad (1)$$

where w is the mass flowrate, p_r reservoir pressure and p_{wf} the well flowing pressure at the depth of the main feedzone (Gudmundsson, 1984).

For cases where Equation 1 holds a graph of mass flowrate vs. the corresponding flowing pressure results in a straight line and the inverse of its slope will be the productivity index. This straight line is the inflow performance for laminar flow. An other characteristic of linear inflow performance is that flowing pressure is bigger than the saturation pressure p_{sat} of the water (Marcou and Gudmundsson, 1986). The upper part of Figure 9 shows this characteristic.

Turbulent Flow

Many geothermal wells do not present lineal behavior above the saturation pressure due to turbulent effects. Several authors have studied this, including Jones and Blount (1976) for gas and oil wells. Gudmundsson (1986) considered the case where the rate of flow from the reservoir into the wellbore is large or the feedzone fracture is narrow, so that the flow may be come turbulent. In this case the linear productivity index should not be used. Other inflow functions are more appropriate to describe turbulent effects, for example the two constant equation

$$p_r - p_{wf} = A\, w + B\, w^2 \qquad (2)$$

where A is the laminar flow (or Darcy) coefficient and B a turbulent coefficient. Dividing through by w gives

$$\frac{p_r - p_{wf}}{w} = A + w\, B \qquad (3)$$

which indicates the reciprocal of the productivity index. When plotted against production rate, a straight line is expected. The slope of such a line a measure of the degree of turbulence.

Two-Phase Flow

Two-phase geothermal wells can have a liquid only or a steam water mixture feedzone. When liquid water (brine) flows into the casing of well, the water will remain liquid up the well until reaching a depth where the pressure is the same as the saturation pressure. At this depth the liquid water will start to flash to form steam. It will continue to flash until reaching the wellhead (Gudmundsson, 1984).

Two-phase feed can result from several reservoir-wellbore flow conditions: it could be liquid water that flashes as it flows toward the wellbore, it could be that the overall fluid state in the reservoir is two-phase, or the well could have two feedzones one of which has liquid feed and the other steam (Gudmundsson, 1986).

When two phases are present the slope of inflow performance curve, below the saturation pressure, becomes more and more negative. This indicates that below the saturation pressure, decrease in p_{wf} becomes less effective at increasing the mass rate into the well (Marcou, 1985).

Marcou and Gudmundsson (1986) stated that at relatively high flowrate the relationship $w/(p_r-p_{wf})$ is likely to become non-liner. This problem was investigated by Vogel (1968) for solution-gas drive hydrocarbon reservoirs. Marcou and Gudmundsson, (1986) utilized Vogel's equation with some modifications for the inflow performance below the saturation pressure when there are two phase and effects of turbulent flow. For this situation the relationship takes the form

$$P.I. = \frac{w}{p_r - p_{wf}} = \frac{2\pi kh}{\mu\nu}\left(\frac{1}{\ln r_r/r_w}\right) \qquad (7)$$

Productivity indexes were calculated from typical values of different geothermal fields, these are given in Table 5. The 13-3/8 in. casing with the inner radius of 158 mm was used for calculating. The reservoir radius was selected equal 100 m after having compared the effect with 10 m and 1000 m, but significative results were not observed when equation (9) was used. The μ and ν values were considered at reservoir temperature. Productivity indexes results are given in the Table 5.

Svartsengi Wells

Theoretical inflow performance of well 12 was determined. Productivity index from Gudmundsson (1984) was used for the linear inflow performance. It was used equaled 26.42 kg/s MPa and below the saturation pressure Equation 5 was utilized to know Δw_{max} and later Equation 4 was applied to calculate the profile, it is shown in Figure 10.

Inflow performance curve, in Figure 10, was compared with other which productivity index was obtained with the pseudosteady-state solution, Equation 7, and it used kh value reported by Gudmundsson (1987). Figure 11 show both inflow performance curves. It a big different can be observed between them due to the kh value is very big and in consequence the productivity index is big too.

Cerro Prieto Wells

The Cerro Prieto reservoir is considered liquid-dominant and high temperature (300-350°C) and pressure and homogenous geologically. Most initial reservoir mesurements temperature fall close to the boiling-point. Some boiling occurs in the

reservoir. In Cerro Prieto wells are found examples of the three different types of inflow performance curves: as linear flow, turbulent flow and two-phase flow.

Data from Iglesias et al. (1983) was considered in this work. They utilized data from wells M-93, M-102, E-2 and M-110 output curves, these relate mass flowrate vs. wellhead pressure, and Iglesias et al.(1983) obtained the flowing pressure using a wellbore simulator reported by Goyal et al. (1980). Figures 12, 13, 14 and 15 of the wells M-93, M-102, E-2 and M-110 show these curves respectively. The saturated pressure in these graph are equivalents to the average reservoir temperatures of the different zones where the wells are located.

M-93 well data are above of saturation pressure, in liquid phase. The terms the $(p_r-p_{wf})/ w$ vs. w are plotted, Figure 16. The straight line that passes through zero can be interpreted that flow is dominated by turbulent effects only.

The same procedure was done for well M-110, and is shown Figure 17. It show certain linearly. The best fit equation shows mainly linear effects and low turbulent effects.

Wells M-102 and E-2 present data above and below the saturation pressure, Figures 14 and 15 show that. The graphs of $(p_r-p_{wf})/w$ vs. w were done only with data above the saturation pressure for each well. The best fit equation of well M-102 show only turbulent effects, Figure 18. Well E-2 best fit equation show turbulent and linear effects, Figure 19.

M-102 and E-2 inflow performance curves below the saturation pressure were fitted utilizing Equation 4. In this Δw_{max} was calculated with Equation 5. In this equation the gradient dp/dw should be known before. In this case Equation 2 can be used, as follow:

$$dp/dw = A + 2\,B\,w \qquad (8)$$

If Equation 8 is substituted in to Equation 5

$$\Delta w_{max} = \frac{p_{sat}}{1.8\,(A + 2\,B\,w)} \qquad (9)$$

The w value was considered at saturation pressure, A and B values are constants obtained in the best fit equation in the graphs of $(p_r - p_{wf})/w$ vs. w.

Figures 20 and 21 show data and 4 possible curves of inflow performance of wells M-102 and E-2 respectively. Square symbol curve is uses the best fit equation for all the data. Triangle symbol curve is utilizes the best fit equation from the data above saturation the pressure. Rohmbus symbol curve present the profile using Equation 4 when the gradient (dp/dw) is obtained from the eqution for all the data and cross symbol curve is when the gradient (dp/dw) is obtained from the equation of the data above of saturation pressure.

In the case of Cerro Prieto the inflow performance curves obtained with the productivity index calculated with Equation 7 was compared with the output data of the wells M-102 and M-110. Figures 22 and 23 shown these respectively.

A productivity index of 24.12 kg/s.MPa calculated with kh= 3.0 m^3 showed a good fit for the well M-110 and with well M-102 only in the first two points, in these the turbulent effects are not present. The result obtained show that the psoudosteady-state solution gives good fit for homogeneous reservoir as Cerro Prieto and bad fit for fractured reservoir as Svartsengi.

RESERVOIR PERFORMANCE

Reservoir performance describes the decrease in reservoir pressure with time as fluid is produced. Reservoir behaviour can be forecast through mathematical model if the production and pressure history are know. The forecast must be linked with wellbore and reservoir performance to determined the field deliverability.

Types of Models

There are two general types of reservoir modeling: numerical simulation and lumped parameter. In numerical simulations, the reservoir system is divided into small blocks having its own properties, and finite difference forms of the governing equations are used to calculate the time and space variation of pressure, mass and enthalpy (Brock, 1986).

Modelers thus attempt to incorporate as much of the reservoir as they consider appropriate. This limits the model validity, since usually most of the required parameters are not known. Geothermal reservoir are usually fractured. In fact, the permeabilities of most reservoir are still largely unknown. This limitation on data means that many of the reservoir elements parameters can only be estimated, using the experience of the modeler and the field engineers, and must be adjusted to obtain a match with the actual reservoir behaviour (Grant et al. 1982).

Lumped-Parameter Models

In lumped-parameter models, average values of fluid and flow properties are assumed throughout the reservoir, and analytic solutions are derived (Brock, 1986).

A reservoir can be confined or unconfined, depending on how it is connected to the surrounding. In a confined system the reservoir volume is fixed and fluid is produced due to

expansion; in unconfined system the reservoir has pressure connection to the surface and fluid production corresponds to water level decline (Gumundsson and Olsen, 1987).

A lumped parameter model is a material balance on a closed reservoir producing an amount of fluid which causes a pressure drop in the reservoir. Both oil and geothermal fields are often connected to a supporting aquifer, however, which adds an influx term to the material balance. Many authors in the petroleum literature have modeled this situation for different geometries and conditions (Brock, 1986).

Water Influx Models

A water influx model is one type of a lumped parameter model. It can be used when the drawdown history of a geothermal reservoir can not be explained by simple mass removal because there may be water influx or recharge into the reservoir. Recharge will maintain pressure in the reservoir, by replacing the produced fluid by usually colder fluids. A term of influx mass has to be added to the mass balance equations for such a reservoir (Olsen, 1984).

Gudmundsson and Olsen, (1985) used a lumped-parameter material-balance model and several water-influx models (Schilthuis, Fetkovitch and Hurst) to match the production history of the Svartsengi geothermal field in Iceland. They found the best results were obtained with the Hurst Simplified model. The method is to take a material balance on the reservoir and to apply the solution of the diffusivity equation in the LaPlace space to account for water influx from the aquifer. The "simplification" is that by using the LaPlace transformation, an expression for drawdown as an explicit function of production rate and the time is found. A parameter containing the ratio of aquifer to reservoir compressibility is central to this derivation (Brock, 1986).

The geometry can be radial or linear. For this work, a radial form was employed. In this case, the reservoir is radial and the supporting aquifer is also radially symmetric layer, infinite in extent, which some of the same properties as the reservoir. The aquifer provides recharge to the reservoir only along the radial edge of the reservoir cylinder. There is no flow into the reservoir through the bottom surface or the top, (Marcou, 1985). The following drawdown solution exists for an infinite radial aquifer:

$$\Delta p = \frac{\mu_a}{2\pi k h \rho_a} \Sigma \Delta w_j [\sigma N(\sigma, t_D - t_{Dj})] \tag{10}$$

where

$$\sigma = (2c_a\rho_a)/(c_r\rho_r) \tag{11}$$

and

$$N(\sigma, t_D - t_{Dj}) = L^{-1}\left[\frac{K_o(\sqrt{s})}{s^{3/2}\,[\sigma K_1(\sqrt{s}) + (\sqrt{s}) K_o(\sqrt{s})]}\right] \tag{12}$$

where $t_D = kt/\varphi\mu_a c_a r_r^2$ for t equal t_n.

A special case of the general radial solution is for large σ. In the limit the drowdown is,

$$\Delta p = \frac{\mu_a}{2\pi k_a h \rho_a} \Sigma \Delta w_p p_D(t_D - t_{Dj}) \tag{13}$$

where $p_D(t_D)$ is the line source solution (Earlougher, 1977)

$$p_D(t_D) = \frac{1}{2} Ei\left(\frac{1}{4t_D}\right) \tag{14}$$

Equation 14 may be approximated

$$p_D = 1/2[\ln(t_D) + 0.80907] \quad (15)$$

when $t_D \geq 25$

The physical interpretation of using the line source solution is that the reservoir is small compared to the aquifer, so the reservoir response is negligible compared to the aquifer drawdown response (Brock, 1986). For this work the line source solution was also utilized for matching the history of the Svartsengi geothermal field.

Field Data

Pressure drop data were taken from the pressure logs obtained by The National Energy Authority of Iceland (G. Gudmundsson, 1988) in wells 5, 6, 7, 8, 9, and 11. These data are presented in the Tables 7-12 and are for 700 m depth. The initial pressure with was considered that in the well 5, in July 7, 1977 as 5.72 MPa, before the reservoir was exploited commercially. The pressure of each well was adjusted to this initial pressure to obtain drawdown with time. A best fit equations was obtained, it is $\Delta p = -1.2771+0.001827\ t-4.228E-7\ t_2 +3.7139E-11\ t^3$. The fit is shown in Figure 24.

Accumulative mass production was obtained from Vatnaskil Ltd. (1985). The average flowrate vs. time (days) is shown in Figure 25. The initial date was considered October 18, 1976. The average flowrate was obtained the accumulative mass at date considered (the end of each year approximately) minus accumulative mass at the end of the year before, divided by time in seconds.

The drawdown and average flowrate are given in Table 13. Graphs of time (days) and accumulative production vs. drawdown were calculated with the best fit equation, these

are presented in Figures 26 and 27, respectively. The data from Table 13 were used to obtain the best fit with the radial Hurst and line source solution models. The data were considered first at 1166 days, when the first drawdown measurement was made.

Hurst Model

A Fortran 77 code from Brock (1986) was utilized to solve the equations of the radial Hurst and line source solution models. In the Hurst model the function is not given analytically in real space, so it must be numerically inverted using the Stehfest Algoritm. This code has two programs one two find the standard deviation and the least-squares slope for a given σ, and one which prepares the model and actual drawdown graphs for a given σ and least square slope.

Brock's code needs values for a permeability and reservoir area. The area value was considered based on 6 km^2. It was reported by Gudmundsson and Olsen (1987) from Georgsson and Tulinius (1983). They estimated this value base a resistivity measurements. These were converted into approximate subsurface temperatures, taking 200°C at 600 m depth as the top of the reservoir. The area estimated for the central part of the reservoir was between 6 and 7 km^2.

The permeability-thickness (kh) was calculated using Equation 7 for pseudosteady-state and the productivity index (26.49 kg/MPa.s.) reported by Gudmundsson (1984). The value obtained was 4.44 E-12 m^3. This is lower than others kh reported in Table 6. The effective reservoir thickness was assumed equal 100 m. Therefore, reservoir permeability was estimated equal to 0.0444 E-12 m^2.

The history match method suggested by Gudmundsson and Olsen (1987) was used in this work. It consists of plotting

$$x(n) = \Sigma\, \Delta w_j \sigma N(\sigma, t_D - t_{Dj}) \qquad (16)$$

vs.

$$y(n) = \Delta p/\rho g = \Delta h(n) \qquad (17)$$

and the slop m from the least squares fit is

$$m = \frac{\mu_a}{2\pi kh\rho_a} \qquad (18)$$

where kh is the permeability-thickness product of the reservoir/aquifer boundary. The fitting procedure is: (1) select a value for σ (2) calculate x(n) and y(n) (3) find the slope m (4) calculate the standard deviation (5) select a new σ value and repeat above steps (6) plot standard deviation vs. σ, and (7) select σ giving the minimum standard deviation, which in turn gives the best match. The compressibility can be determined from σ.

Several runs were done with the Hurst model. The slope value was substituted to in Equation 18 to calculated the permeability-thickness (kh) product. Sigma (σ) was substituted in Equation 11, to obtain the compressibility and the storativity of the reservoir. Reservoir temperature was considered 240°C and the aquifer temperature 100°C water density values. The aquifer compresibily was considered as 5.0E-10 Pa^{-1}. Results of all these parameters are given in Table 14.

Line Source Solution Model

The Fortran 77 code from Brock (1986) was utilized to solve the equations of the line source solution model. This code has a program which prepares the match results and forecast.

The input data necessary for running the program are drawdown pressure, mass flowrate and time as given in Table 13. The permeability and reservoir area values are the same as for Hurst model were considered. The results are presented in Table 14.

Forecast of the Models

Production data used in this work cover a period of more than 11 years (4206 days). A prediction for the next 4000 days was done for both models. Tables 15 and 16 show the Hurst model and line source solution model results respectively. Time (days) and accumulative mass produced vs. drawdown with real data and the best fit prediction for the Hurst model are shown in Figures 28 and 29 respectively. The same was done for the line source solution model as presented in Figure 30.

FIELD DELIVERABILITY

Deliverability is the overall effect of the three performances: reservoir, inflow and wellbore. When the wellbore performance and the inflow performance curves are plotted together their intersection determines the production rate of a well. As production continues, the reservoir pressure will decrease. The water influx model, in this case the Hurst simplified model, provides the new reservoir pressure. At the new conditions the wellbore performance curves look the same since the assumption of constant enthalpy fluid production has been made and all other factors for the well remain unchanged. However, the inflow performance curve will change. As before, the inflow performance curve is constrained to pass through the reservoir pressure. The productivity index, or slope of the inflow performance curve, does not depend upon the reservoir pressure. Consequently, the inflow performance curve will shift downwands so that it is parallel to the old curve but passes through the new reservoir pressure.

The method to estimate future production from a geothermal field deliverability consists of:

1.- Take the wellbore performance curve as constant, because the casing and liner of a well do not change in the time.

2.- A reservoir model gives future drawdown. A new reservoir pressure might be obtained with

$$p_{nr} = p_{ir} - \Delta p \qquad (19)$$

where p_{nr} is the new reservoir pressure, p_{ir} is initial reservoir pressure and Δp is the drawdown pressure has have the reservoir.

3.- This new reservoir pressure can be used with linear flow, turbulent flow or two phases inflow performance

equations to tray to obtain the inflow performance curves.
4.- These new curves can plotter together with the wellbore performance curves and know the future deliverability of the reservoir.

An example of deliveravility calculations is presented with well 12 and drawdown pressure forecast in the Svartsengi field. Figure 31 shows the combination of wellbore and inflow performance curves. This figure was done in the follow form.

Wellbore performance curves of well 12 were chosen. In the wellbore performance section, it is explained how the curves were done. The inflow performance curve above of saturation pressure presented in Figure 31, it was calculated using the linear flow equation and the productivity index reported by Gudmundsson (1984), which is 26.42 kg/s.MPa. Inflow performance below saturation pressure was calculated with Equations 4 and 5 for two-phase flow. The others inflow performance curves were calculated assuming the same productivity index and the new pressure estimated with Equation 19 in years 1983, 1986 and 1991.

The wellbore performance curve at 1.0 MPa is taken as the reference. The points at which this curve intersects with the inflow performance curve must be considered the future production rate for this well. It can be observed how the productivity of the well decreases over time. For example,the production rate for year 1991 will be 82 kg/s. Deliverability can be used to estimated futures output-curves from wellhead pressure of each wellbore performance curve and the flowrate determined.

DISCUSSION

Wellbore performance can be considered constant as long as there is no problem of scaling. If scaling occurs the wellbore performance curves will change, but if the casing is cleaned the curves will obtain their initial values. In the case where the casing has to be changed due to collapse or rupture, with a different diameter to the previous one, then new curves have to be calculated. The casing diameter is the only actor that can be optimize for new wells in a geothermal field. This can be done with a wellbore performance study as explained by Marcou and Gudmundsson (1986).

The inflow performance curve is a composite of two forms of flow behavior, one above saturation pressure and other below this pressure (Marcou, 1985). Above the saturation pressure the flow might be dominated by laminar effects as postulated for well 12 of Svartsengi and well M-110 of Cerro Prieto. Other types of wells are M-93 where the turbulent effects are dominant above the saturation pressure. Wells M-102 and E-2 that present turbulent effects above and below of saturation pressure. The inflow performance curve obtained for these equations are approximations that might be utilized, but must take into consideration that the turbulent and two-phase equations suppose an isothermal system.

It is important to know what changes a reservoir will have in the future for establishing a exploition strategy. This can be achieved with the deliverability concept. It should be noted that it is necessary to work with wellbore and reservoir simulators when concept of deliverability is bing used. These tools provide an approximation to the real phenomena.

CONCLUSIONS

1.- Wellbore performance curves in Svartsengi field were calculated using a wellbore simulator at different wellhead pressures.

2.- The wellbore performance of a well can be defined by a straight line when flowing below the saturation pressure by plotting the square root of the difference between wellhead pressure and flowing pressure.

3.- Equations for linear, turbulent and two-phase effects are given. These were used to calculate the inflow performance curves of wells in Svartsengi and Cerro Prieto geothermal fields.

4.- The well known pseudo stead-state solution was used to calculated the productivity indexes with typical kh values reported in the literature and these compared with inflow performance curves of wells mentioned before. It was found that pseudosteady-state solution gives better fit for homogeneus reservoir as Cerro Prieto than for fractured reservoir as Svartsengi.

5.- Pressure drawdown matching and forecasting were done for Svartsengi field using Hurst water influx modeling.

6.- The methodology to estimate the deliverabily of a geothermal field is given. One example is presented using the wellbore performance, inflow performance and reservoir performance of well 12 of Svartsengi.

ACKNOWLEDGEMENT

I would like to extend my thanks to the United Nations University and Orkustofnun, National Energy Authority of Iceland, who did all possible for the success of the geothermal training programme.
My thanks to the Gerencia de Proyectos Geotermoélectricos of the Comisión Federal de Electricidad de México for permitting me to attend this training.
Special thanks to Dr. Jón-Steinar Gudmundsson, Director of the institution and my advisor for his patience and advices during develop of this project.
My gratitude to parents and my family, Lorenia, Rodrigo and Gonzalo, whose understanding and encouragement were essential for fishing this training.

NOMENCLATURE

A = Linear coefficient
B = Turbulent coefficient
c = Compressibility (Pa^{-1})
g = Acceleration of gravity (9.81 m/s^2)
h = Height of reservoir (m)
k = Permeability (m^2)
L = LaPlace operator
M,N = Hurst functions
p = Pressure (MPa)
P.I. = Productivity index (kg/s.MPa)
r = Radius (m)
s = Variable in LaPlace space
t = Time (s)
w = Mass rate (kg/s)
μ = Viscosity (MPa.s)
φ = Porosity
ρ = Density (Kg/m^3)
σ = Hurst parameter
ν = Specific volume (m^3/kg)

Subscripts

a = Aquifer
D = Dimensionless
i = Initial
r = Reservoir
sat = Saturation conditions
wf = wellbore fluid

REFERENCES

Alonso E. H., Dominguez A. B. , Lippman M. J., Manon M. A., Shroeder, R.C. and Witherspoon P. A., (1978): "Recent Activities At Cerro Prieto," Fourth Workshop Geothermal Reservoir Engineering, Stanford University, Stanford, California, pp. 5-14.

Bjarnason J.Ö., (1988): Svartsengi Chemical Monitoring 1980-1987,Report OS-88001/JHD-01, National Energy Authority, Reykjavik, pp 8.

Bodvarsson S. G., Pruess K., Stefansson V. and Eliasson E., (1983): "A Summary of Modeling Studies of the Krafla Geothermal Field, Iceland," Geothermal Resources Council, Transactions vol.17, pp. 391-396.

Brock, D.C., (1986): Compressibility Effects in Modeling Two-Phase Liquid Dominated Geothermal Reservoir, Pet. Ing. Dept. Stanford University, 31 pp.

Erlougher R.C., (1977): Advances In Well Test Analysis, SPE, Dallas, pp. 6-14.

Georgsson L. S. and Tulinius H., (1983): "Resistivity Measurements on Outer Reykjanes Peninsula 1981 and 1982," Report OS-83049/JHD-09, Geothermal Div., National Energy Authority, Reykjavík.

Grant M., (1980): "The Testing of KA28- Pressure Analysis in a Two-Phase Reservoir," Sixth Workshop Geothermal Reservoir Engineering, Stanford University, Stanford, California, pp. 170-177.

Grant M., Donaldson I.G. and Bixley P., (1982): Geothermal Reservoir Engineering, Academic Press, Inc., New York, N.Y., pp. 244-246.

Gudmundsson G. (1988): Personal communication, National Energy Authority, Reykiavík.

Gudmundsson J.S., (1984): "Discharge Analysis Method For Two-Phase Geothermal Wells," Transaction Geothermal Resource Council, vol. 8, pp. 295-299.

Gudmundsson J.S., (1986): "Two-Phase Wells," Bulletin, March, Geothermal Resource Council, pp. 10-16.

Gudmundsson J.S. and Olsen G., (1987): "Water-Influx Modeling of Svartsengi Geothermal Field, Iceland," SPE Reservoir Engineering, February 1987, pp. 77-84.

Iglesias E., Arellano V. and Molinar R., (1983): "A Method to Recover Useful Geothermal-Reservoir Parameters from Production Characteristic Curves. Hot Water Reservoirs," Proceedings, Ninth Workshop Geothermal Reservoir Engineering, Stanford University, Stanford, CA., pp. 291-297.

Kjaran S.P., Halldorsson G.K., Thorhallsson S. and Eliasson J., (1979): "Reservoir Engineering Aspects of Svartsengi Geothermal Area" Transactions, Geothermal Resources Council, vol. 3, pp. 337-339.

Lippman J. M., (1982): "Overview of Cerro Prieto Studies," Eighth Workshop Geothermal Reservoir Engineering, Stanford University, Stanford, Californaia, pp. 49-66.

Marcou J.A., (1985): Optimizing Development Strategy For Liquid Dominated Geothermal Reservoirs, Stanford Geothermal Program Report SGP-TR-90,Stanford University, Stanford, CA, 157 pp.

Marcou J.A. and Gudmundsson J.S. (1986): "Development Model for Geothermal Reservoirs," paper SPE 15119 presented at 1986 SPE California Regional Meeting, Oakland, CA, April 2-4, pp. 77-84.

Nind T.E.W., (1981): Principles of Oil Well Production McGraw-Hill Book Company, 2nd Edition, pp. 45-67.

Ortiz J., (1983): Two-Phase Flow in Geothermal Wells: Developmenta and Uses of Computer Code, Stanford Geothermal Program, Report SGP-TR-66, Stanford University, Stanford, CA, 42 pp.

Rivera J., (1978): "Injection Testing in Geothermal Wells," Fourth Workshop Geothermal Reservoir Engineering, Stanford University, Stanford, California, pp. 176-187.
Vatnaskil Ltd., (1985): Svartsengi Field Production 1976-1985, National Energy Authority, Report OS-85097/JHD-12, 99 pp.

Table 1. Casing diameter, casing and main feedzone depth of Svartsengi wells.

WELL	CASING DIAMETER(in)	CASING DEPTH(M)	MAIN FEEDZONE(m)
7	13-3/8	1436	800
8	13-3/8	1609	1300
9	13-3/8	994	900
11	13-3/8	1141	900
12	13-3/8	607	-
12	12-1/4	1488*	1200

* Barefoot

Table 2. Results of wellbore simulator for well 7

WELL HEAD PRESSURE (MPa)abs.	0.7	0.9	1.1	1.2
MASS FLOWRATE (kg/s)	WELL FLOWING BOTTOM PRESSURE (MPa)abs.			
60.0	1.31	1.54	1.82	2.00
80.0	1.54	1.74	2.00	2.16
100.0	1.78	1.96	2.21	2.37
110.0	1.91	2.08	2.33	2.49
120.0	2.04	2.21	2.46	2.63

Table 3. Results of wellbore simulator for well 8

WELL HEAD PRESSURE (MPa)abs.	0.7	0.9	1.1	1.2
MASS FLOWRATE (kg/s)	WELL FLOWING BOTTOM PRESSURE (MPa)abs.			
60.0	1.79	2.15	2.94	3.92
80.0	2.22	2.62	3.70	4.58
100.0	2.83	3.56	4.71	5.36
110.0	-	4.20	5.20	5.78
120.0	4.02	4.83	-	6.19

Table 4. Results of wellbore simulator for well 9

WELL HEAD PRESSURE (MPa)abs.	0.7	0.9	1.1	1.2
MASS FLOWRATE (kg/s)	WELL FLOWING BOTTOM PRESSURE (MPa)abs.			
60.0	1.40	1.63	1.95	2.15
80.0	1.65	1.86	2.16	2.36
100.0	1.93	2.13	2.42	2.64
110.0	2.07	2.27	2.58	2.81
120.0	2.23	2.43	2.79	3.02

Table 5. Results of wellbore simulator for well 12

WELL HEAD PRESSURE (MPa)abs.	0.5	0.6	1.0	1.1
MASS FLOWRATE (kg/s)	WELL FLOWING BOTTOM PRESSURE (MPa)abs.			
50.0	1.36	1.50	3.68	8.02
75.0	1.83	2.02	4.28	7.79
100.0	2.41	2.80	5.21	7.92
125.0	2.82	4.27	6.08	8.29

Table 6. Typical kh values of different geothermals fields and productivity indexes calculated with pseudosteady-state solution.

GEOTHERMAL FIELD	kh (m^3)	T (°C)	P.I. (kg/s.MPa)	REFERENCES
SVARTSENGI	170.0 E-12	240	1231.70	a
	68.0 E-12	240	492.70	b
CERRO PRIETO	3.0 E-12	325	24.15	c
	1.2 E-12		9.65	d
KRAFLA	2.0 E-12	300	15.79	e
LOS AZUFRES	0.96 E-12	240	6.96	f
WAIRAKEI	18.0 E-12	265	136.40	g
	35.0 E-12	265	265.23	h
KAWERAU	1.0 E-12	290	7.82	i

a.- Kjaran et al., (1979).
b.- Gudmundsson and Olsen, (1987).
c.- Alonso et al., (1978).
d.- Lippman, (1982).
e.- Bodvarsson et al., (1983).
f.- Rivera, (1978)
g.- Zais and Bodvarson (1980).
h.- Wooding, (1981).
i.- Grant, (1980).

Table 7. Pressure measures at 700 m depth in well 5 of Svartsengi geothermal field (G. Gudmundsson, 1988)

WELL 5 SVARTSENGI	
DATE YEAR-MONTH-DAY	PRESSURE (AT 700 m DEPTH) (MPa)
1976-07-17	5.72
1977-06-23	5.60
1982-03-18	4.78
1983-05-05	4.51
1984-03-27	4.46
1985-04-24	4.34
1987-05-07	4.12
1987-10-23	4.10

Table 8. Pressure measures at 700 m depth in well 6 of Svartsengi geothermal field (G. Gudmundsson, 1988).

WELL 6 SVARTSENGI	
DATE YEAR-MONTH-DAY	PRESSURE (AT 700 m DEPTH) (MPa)
1980-10-06	5.23
1981-12-09	4.89
1983-06-16	4.39
1984-05-07	4.41
1984-09-17	4.39
1985-04-30	4.36
1985-12-18	4.18
1986-07-10	4.24
1987-05-07	4.45

Table 9. Pressure measures at 700 m depth in well 7 of Svartsengi geothermal field (G. Gudmundsson, 1988).

WELL 7 SVARTSENGI	
DATE YEAR-MONTH-DAY	PRESSURE (AT 700 m DEPTH) (MPa)
1979-10-28	5.40
1979-11-02	5.34
1979-11-23	5.38
1980-12-90	5.43
1980-03-04	5.34
1980-10-08	5.20
1982-03-15	4.74
1983-05-04	4.56
1984-04-30	4.41
1985-04-20	4.38
1986-06-03	4.15
1987-04-29	4.12

Table 10. Pressure measures at 700 m depth in well 8 of Svartsengi geothermal field (G. Gudmundsson, 1988).

WELL 8 SVARTSENGI	
DATE YEAR-MONTH-DAY	PRESSURE (AT 700 m DEPTH) MPa
1980-02-11	5.24
1980-10-08	5.39
1982-03-16	4.71
1983-03-16	4.55
1984-05-02	4.50
1985-04-23	4.31
1987-04-30	4.12

Table 11. Pressure measures at 700 m depth in well 9 of Svartsengi geothermal field (G. Gudmundsson, 1988).

WELL 9 SVARTSENGI	
DATE YEAR-MONTH-DAY	PRESSURE (AT 700 m DEPTH) (MPa)
1980-10-08	5.11
1982-03-17	4.77
1983-05-04	4.54
1984-04-13	4.51
1987-04-27	4.09
1987-11-14	4.09

Table 12. Pressure measures at 700 m depth in well 11 of Svartsengi geothermal field (G. Gudmundsson, 1988).

WELL 11 SVARTSENGI	
DATE YEAR-MONTH-DAY	PRESSURE (AT 700 m DEPTH) (MPa)
1980-11-27	5.17
1982-03-18	4.75
1985-12-11	4.19
1987-04-29	4.08

Table 13. Input data from Svartsengi geothermal field to Radial Simplified Hurst model and Line Source Solution model. G. Gudmundsson, (1988) and Vatnaskil Ltd., (1985).

DATE YEAR-MONTH-DAY	TIME (days)	DRAWDOWN (MPa)	FLOWRATE (kg/s)
1976-10-18	0	0.00	0.00
1979-12-26	1166	0.34	60.55
1980-12-29	1529	0.66	80.10
1981-12-26	1890	0.92	110.00
1982-12-18	2237	1.11	131.70
1983-12-27	2599	1.27	148.10
1984-12-31	3333	1.50	173.70
1985-12-31	2698	1.57	187.70
1987-12-31	4060	1.66	197.50
1988-12-26	4209	1.69	201.50

Table 14. Results obtained with the Hurst and line source solution

MODEL	kh (m^3)	c_r (Pa^{-1})	Sp (m/kPa)
Hurst	30.8 E-12	0.53 E-6	2.692 E-3
Line Source	30.9 E-12		

Table 15- Results of Hurst model.

Geothermal field : Svartsengi

Permeability.....: .444000E-13(m2)
Porosity.....: .0500
Area.....: 6.0000(km2)

time (days)	flowrate (kg/s)	drawdown(real) (MPa)	drawdown(calc.) (MPa)
0.	0.0000	0.0000	0.0000
1166.	60.5000	.3400	.2899
1529.	142.8400	.6600	.5685
1890.	236.6100	.9200	.9613
2237.	249.8300	1.1100	1.1479
2599.	249.7100	1.2700	1.2493
2964.	261.2900	1.3900	1.3526
3333.	266.6100	1.5000	1.4310
3698.	316.1500	1.5700	1.6380
4063.	296.4900	1.6600	1.6652
4209.	313.1300	1.6900	1.7090
4357.	308.5900	-	1.7340
4505.	306.0700	-	1.7503
4653.	309.2633	-	1.7714
4802.	307.9744	-	1.7872
4950.	307.7693	-	1.8011
5098.	308.3357	-	1.8154
5246.	308.0265	-	1.8280
5394.	308.0438	-	1.8399
5542.	308.1353	-	1.8513
5690.	308.0685	-	1.8619
5839.	308.0825	-	1.8720
5987.	308.0955	-	1.8818
6135.	308.0822	-	1.8911
6283.	308.0867	-	1.8999
6431.	308.0881	-	1.9085
6579.	308.0857	-	1.9167
6728.	308.0868	-	1.9246
6876.	308.0869	-	1.9323
7024.	308.0865	-	1.9397
7172.	308.0867	-	1.9468
7320.	308.0867	-	1.9537
7468.	308.0866	-	1.9605
7616.	308.0867	-	1.9670
7765.	308.0867	-	1.9734
7913.	308.0867	-	1.9796
8061.	308.0867	-	1.9856
8209.	308.0867	-	1.9914

Minimum standard deviation is : 5.068526763513116E-02
resulting from sigma as .....: 3.630780547701015E-02
Slope.....: 1.520025809843953E-03

Table 16- Results of Line Source Solution model.

Permeability.....: 4.44000E-14m2
Porosity.....: 5.00000E-02
Area.....: 6.0km2

Time(days)	Cum.(Mkg)	Drawdown (MPa) real	Drawdown (MPa) calc.
.00000E+00	.00000E+00	.00000E+00	.00000E+00
1166.0	6094.9	.34000	.29383
1529.0	10575.	.66000	.63734
1890.0	17955.	.92000	1.0643
2237.0	25445.	1.1100	1.1918
2599.0	33255.	1.2700	1.2488
2964.0	41495.	1.3900	1.3377
3333.0	49995.	1.5000	1.3988
3698.0	59965.	1.5700	1.6324
4063.0	69315.	1.6600	1.6051
4209.0	73265.	1.6900	1.6731
4574.0	83140.	-	1.7152
4939.0	93015.	-	1.7458
5304.0	.10289E+06	-	1.7716
5669.0	.11276E+06	-	1.7941
6034.0	.12264E+06	-	1.8143
6399.0	.13251E+06	-	1.8327
6764.0	.14239E+06	-	1.8495
7129.0	.15226E+06	-	1.8651
7494.0	.16214E+06	-	1.8796
7859.0	.17201E+06	-	1.8932

Standard deviation.. : 7.12549E-02
Slope..... : 1.41530E-03

program : linesource

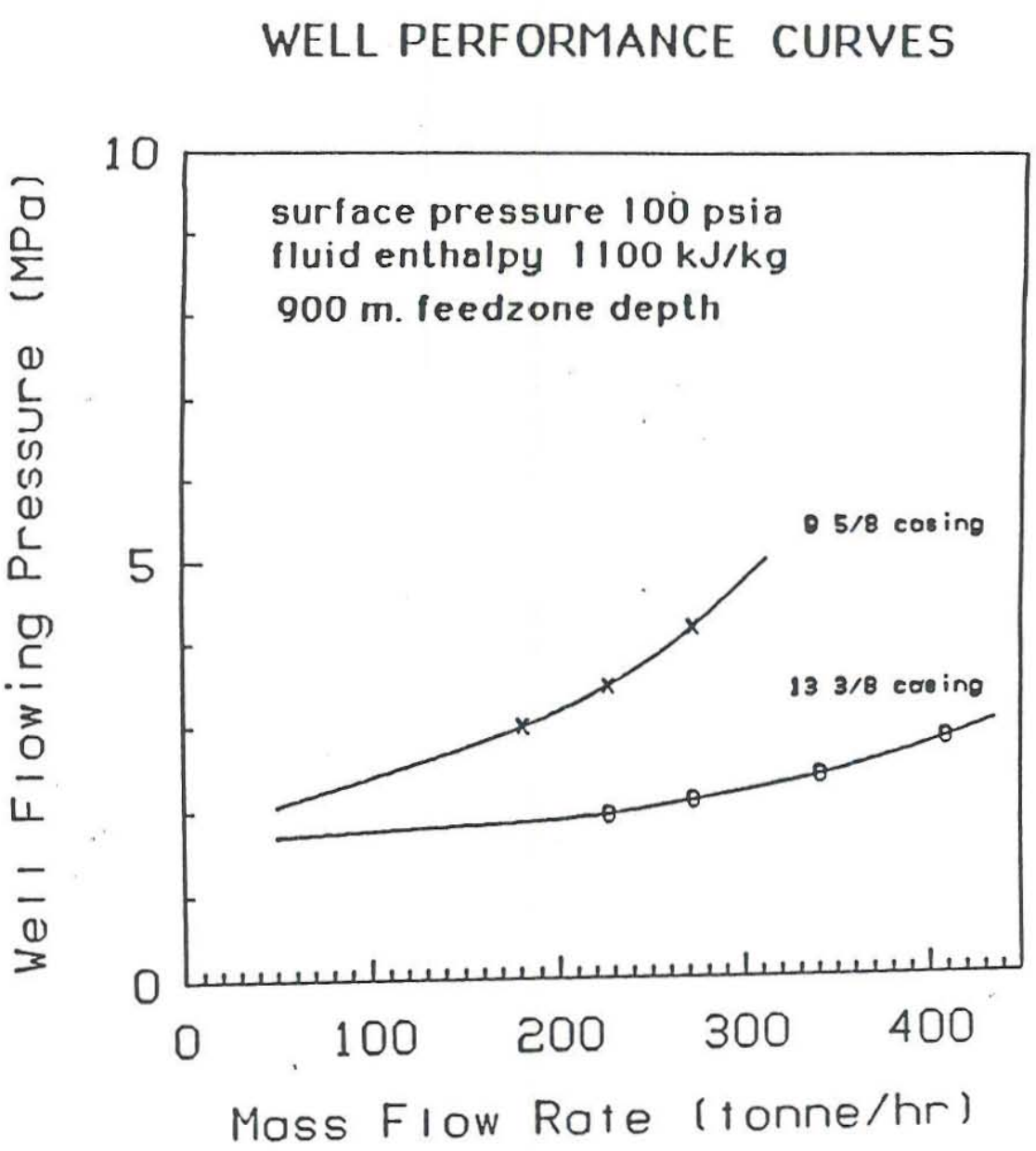

Figure 1- Wellbore performance curves with 9-5/8 in. and 13-3/8 in. casings (Marcou, 1985)

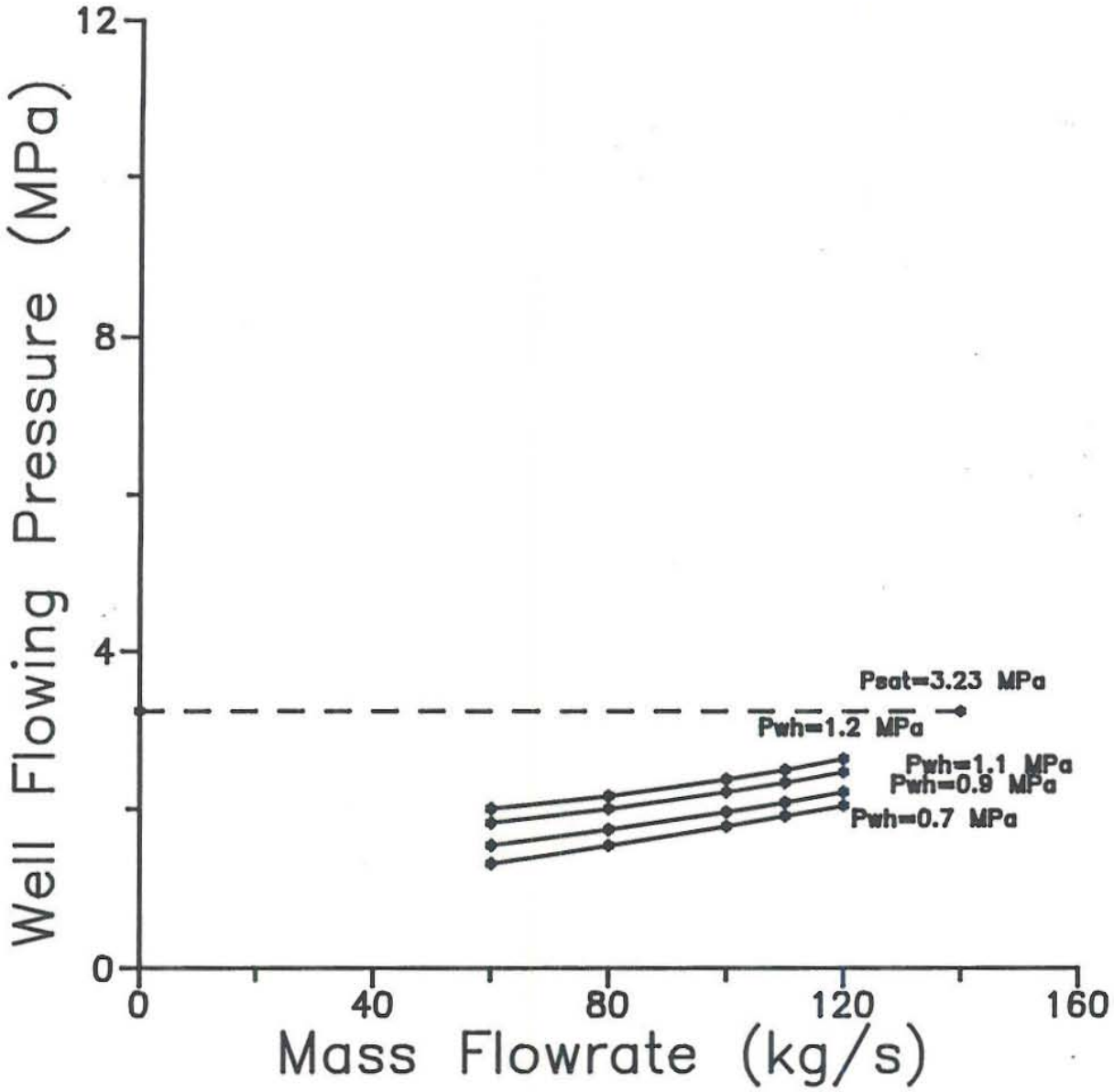

Figure 2- Wellbore performance curves Well 7 of Svartsengi at different wellhead pressures.

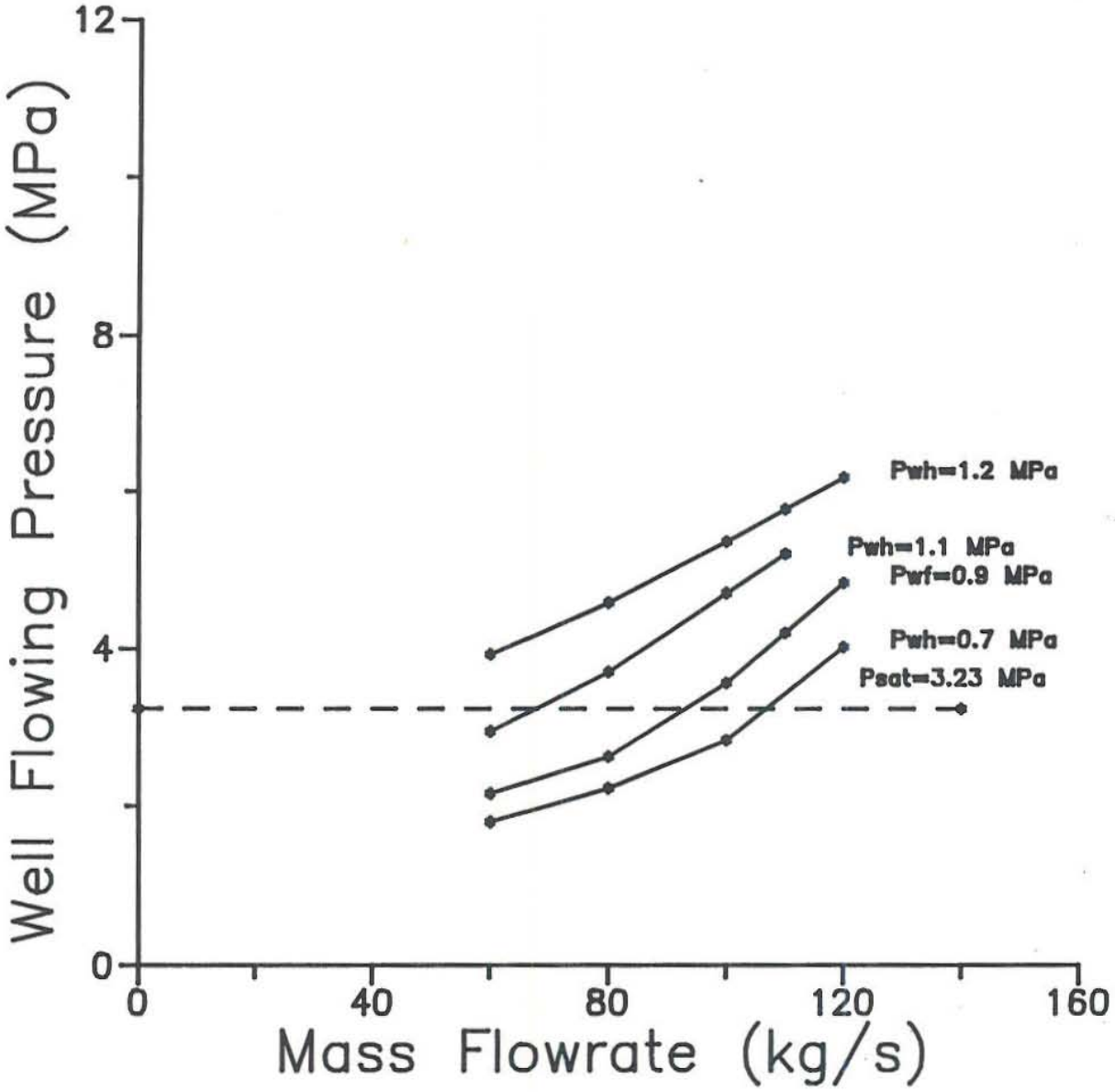

Figure 3- Wellbore performance curves Well 8 of Svartsengi at different wellhead pressures.

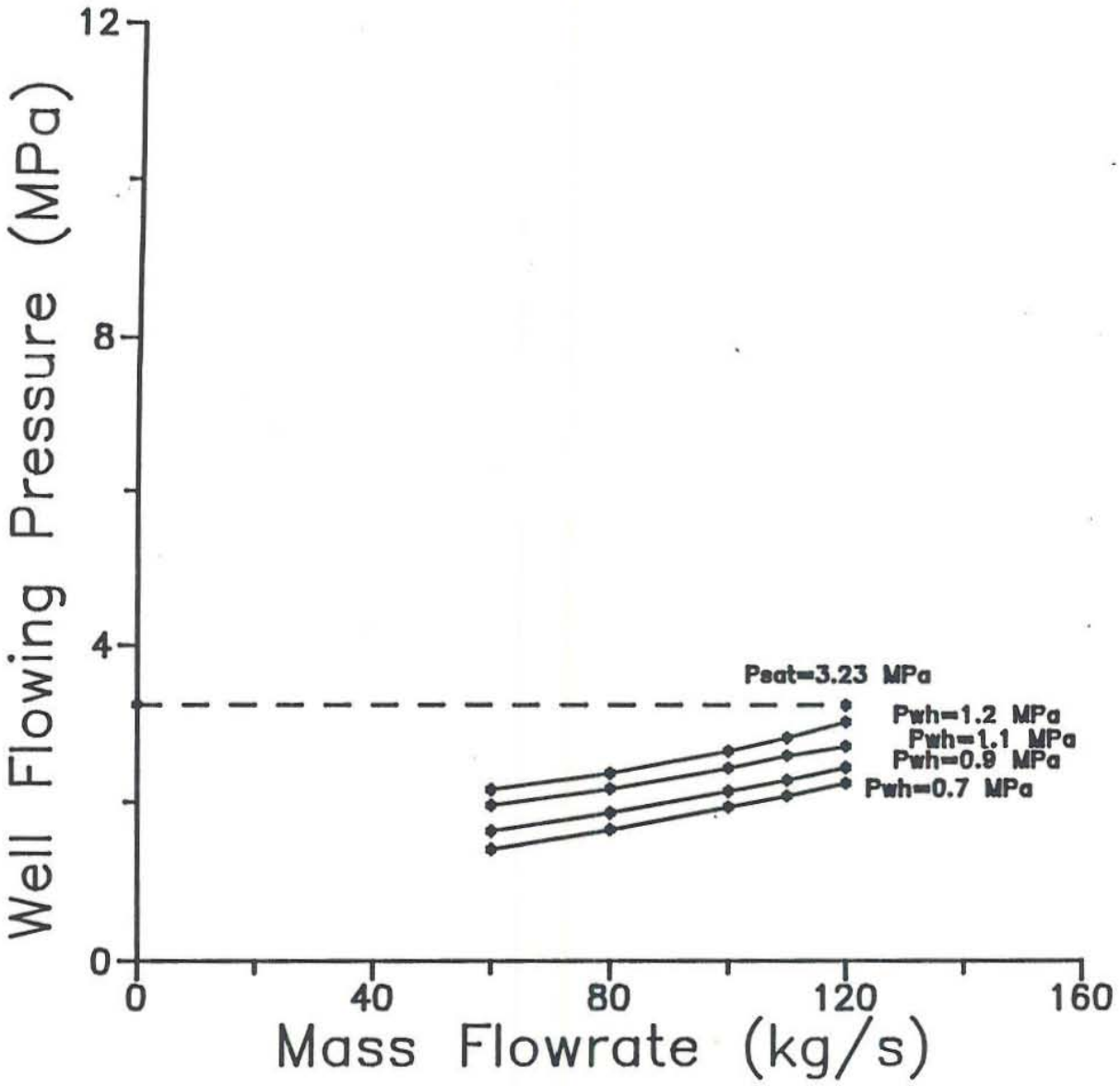

Figure 4- Wellbore performance curves Well 9 of Svartsengi at different wellhead pressures.

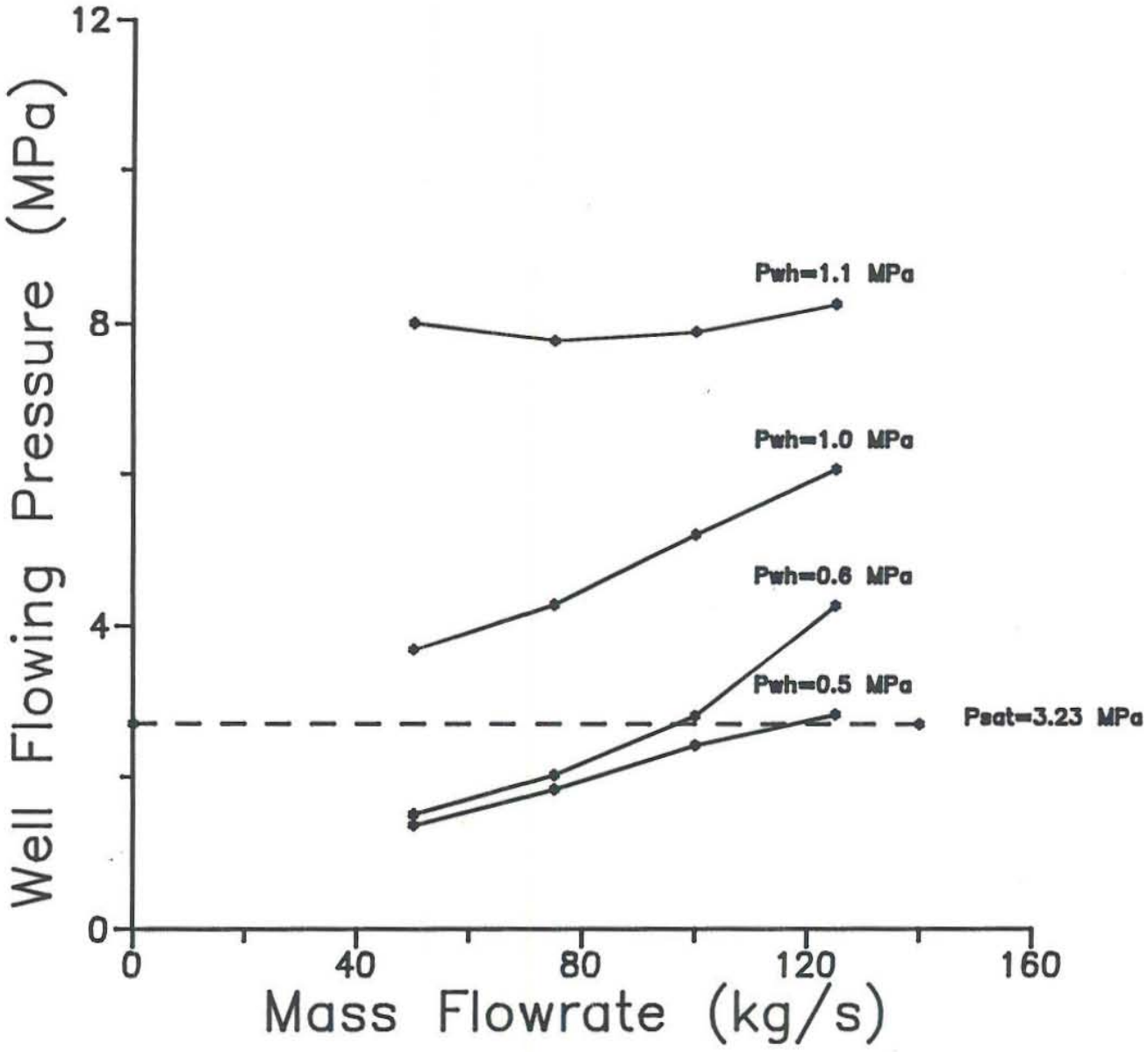

Figure 5- Wellbore performance curves Well 12 of Svartsengi at different wellhead pressures.

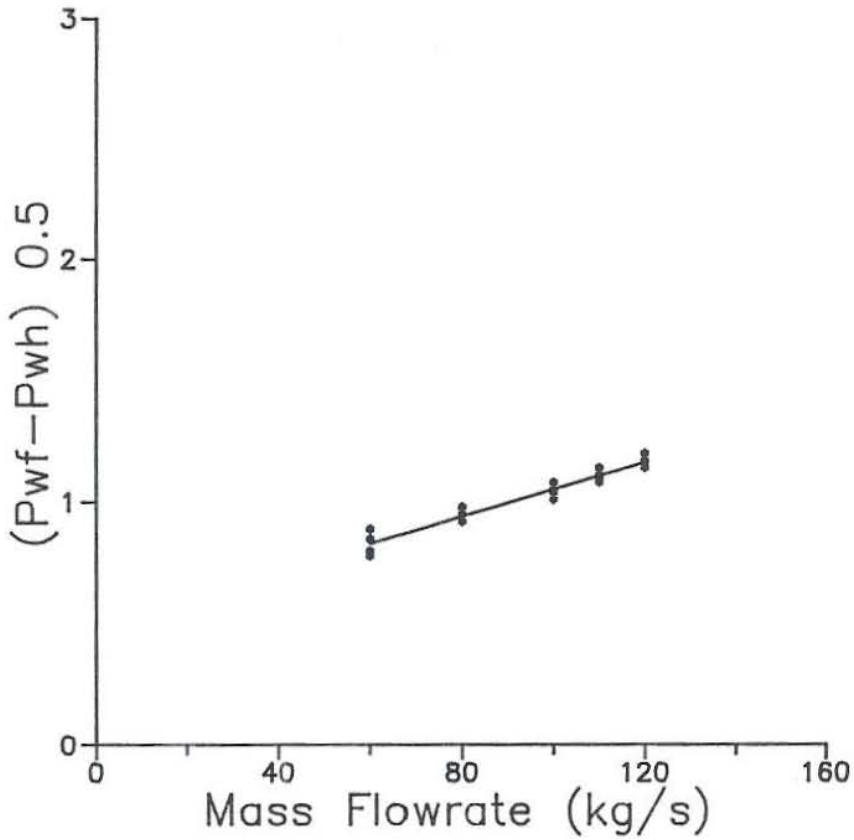

Figure 6- Straight line Well 7 of Svartsengi at pressures below saturation pressure.

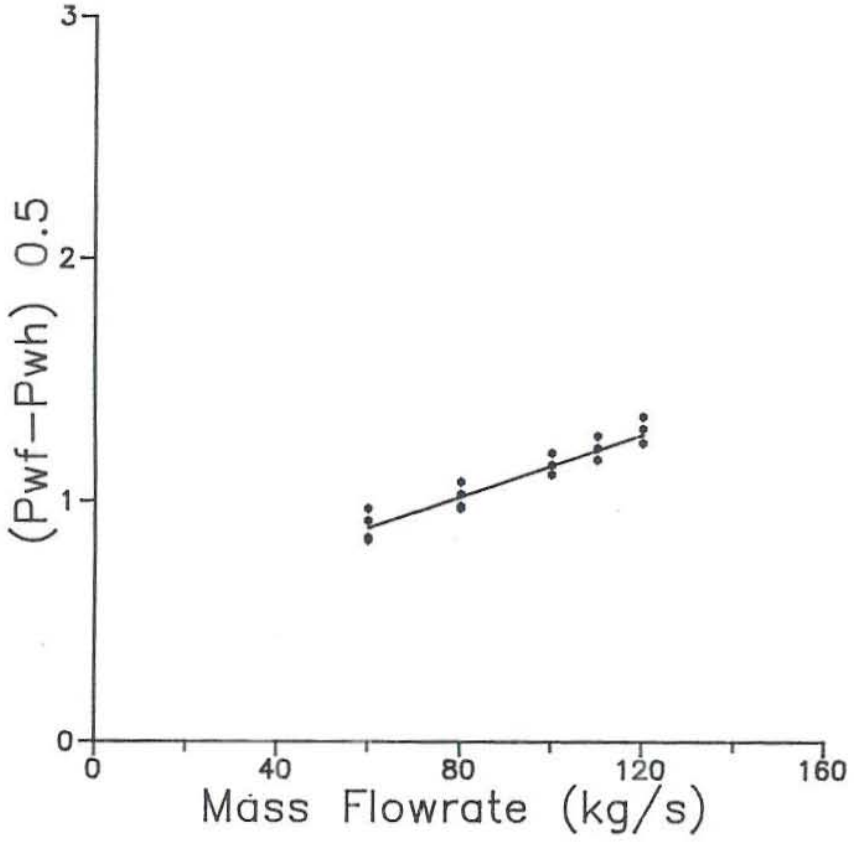

Figure 7- Straight line Well 9 of Svartsengi at pressures below saturation pressure.

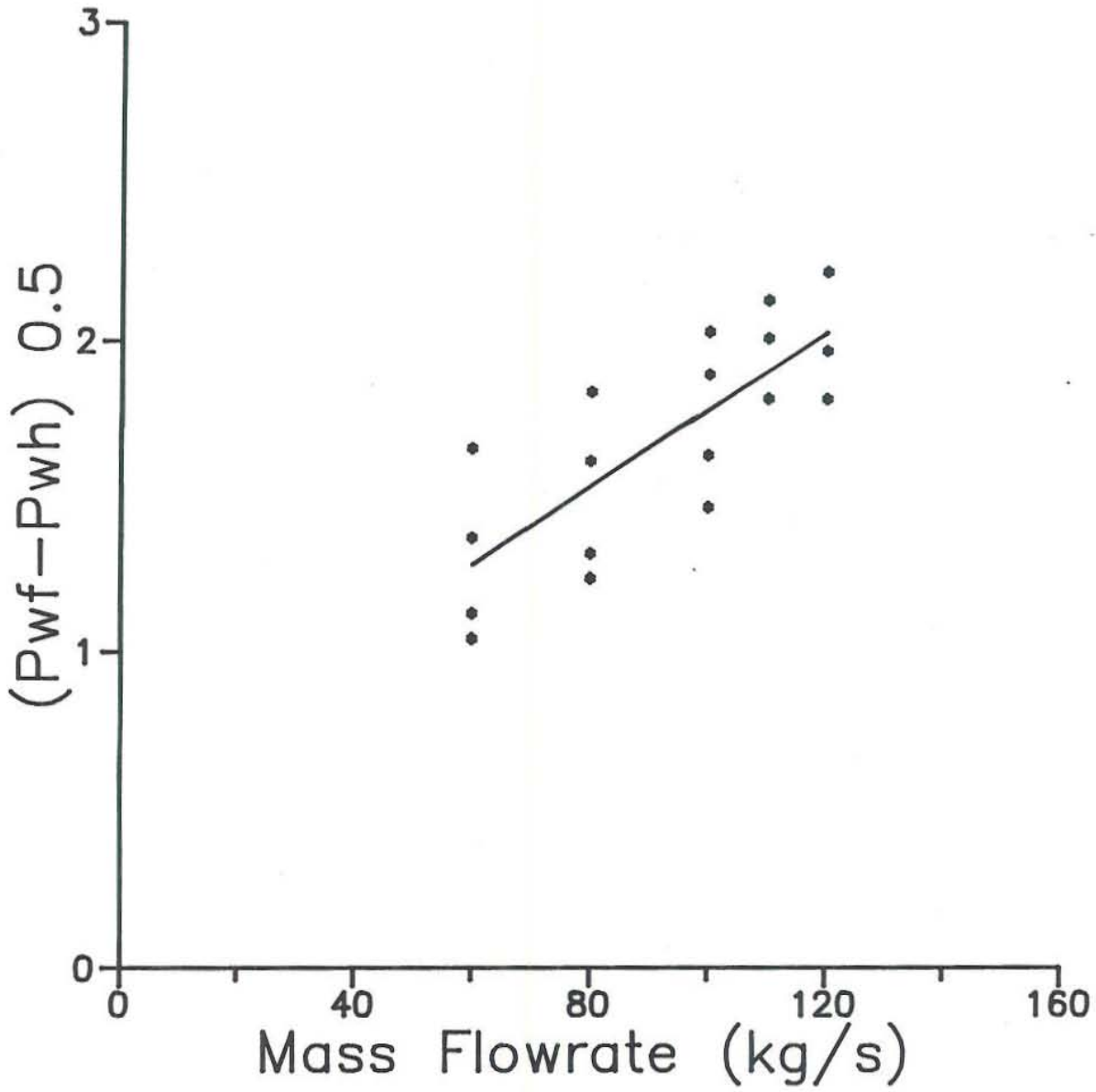

Figure 8- Bad fit Well 8 of Svartsengi at pressures below saturation pressure.

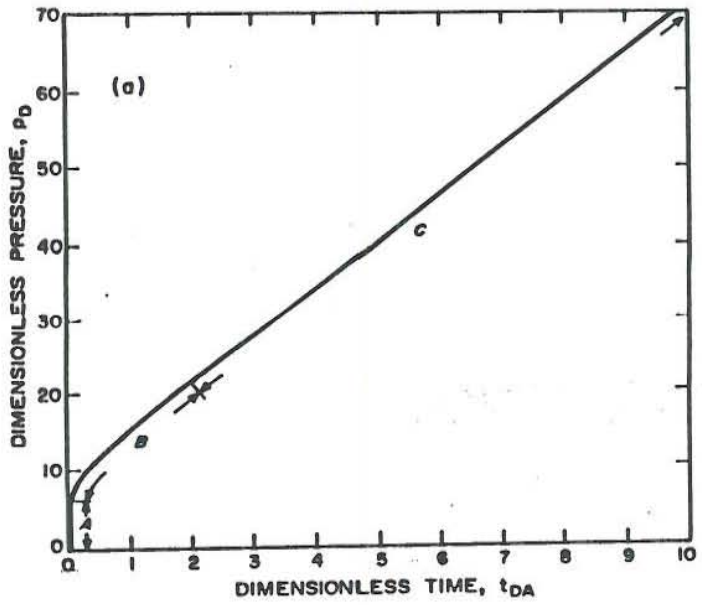

Figure 9- Transient flow regimens: A-infinite acting; B-transition; C-pseudosteady-state (Erlougher, 1977).

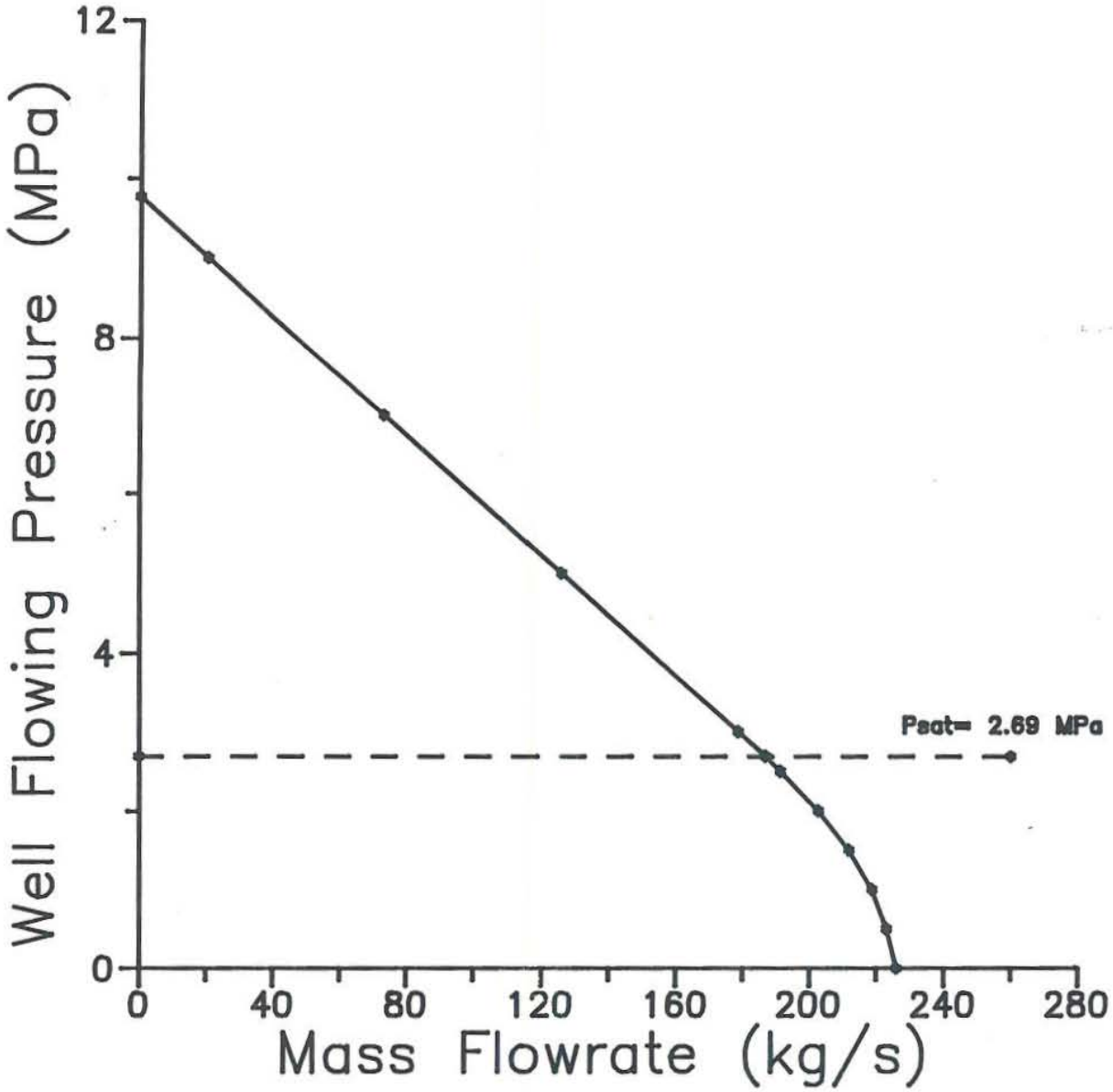

Figure 10- Inflow performance curve Well 12 of Svartsengi.

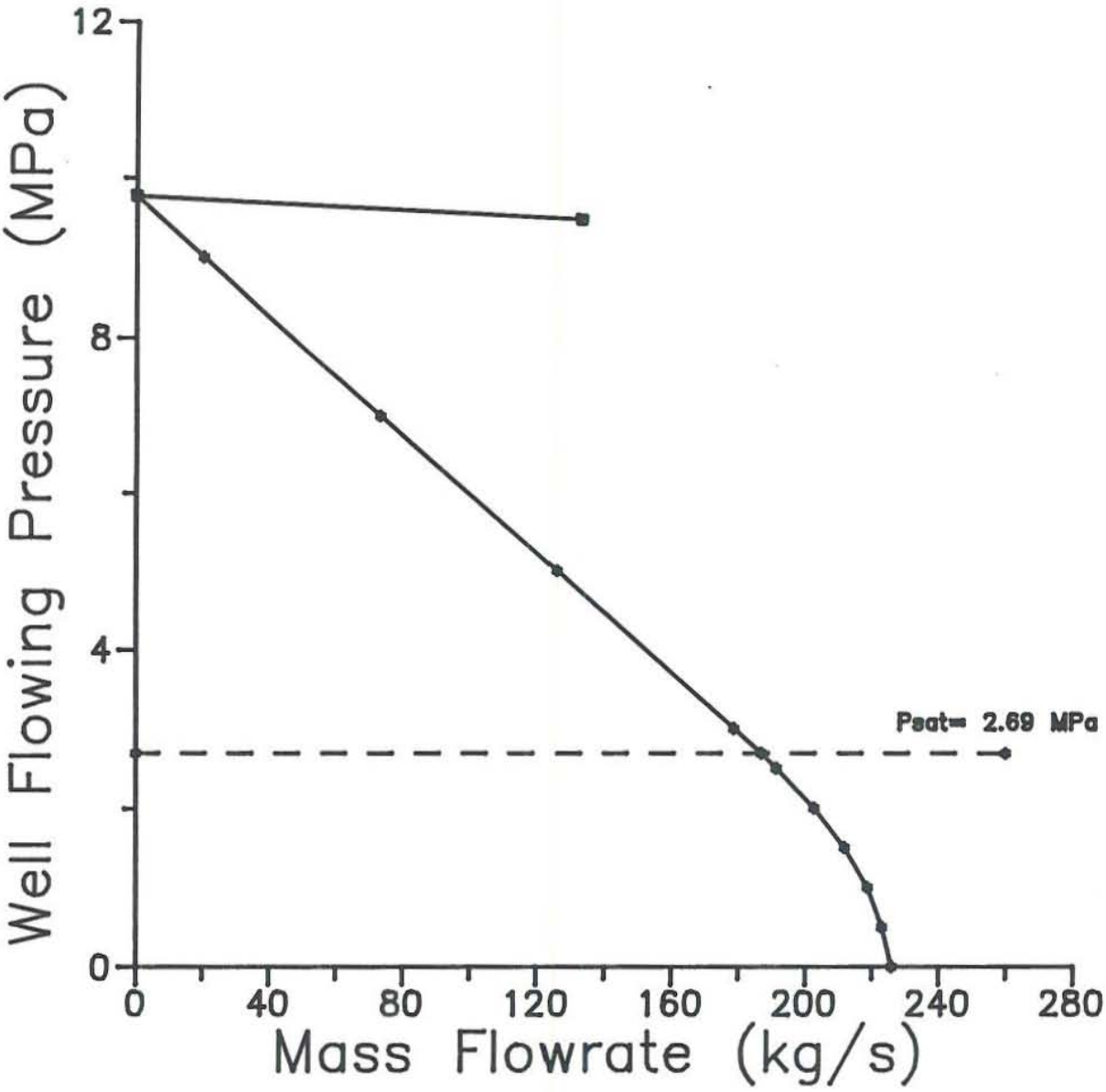

Figure 11- Comparatione of inflow performance curves Well 12 of Svartsengi.

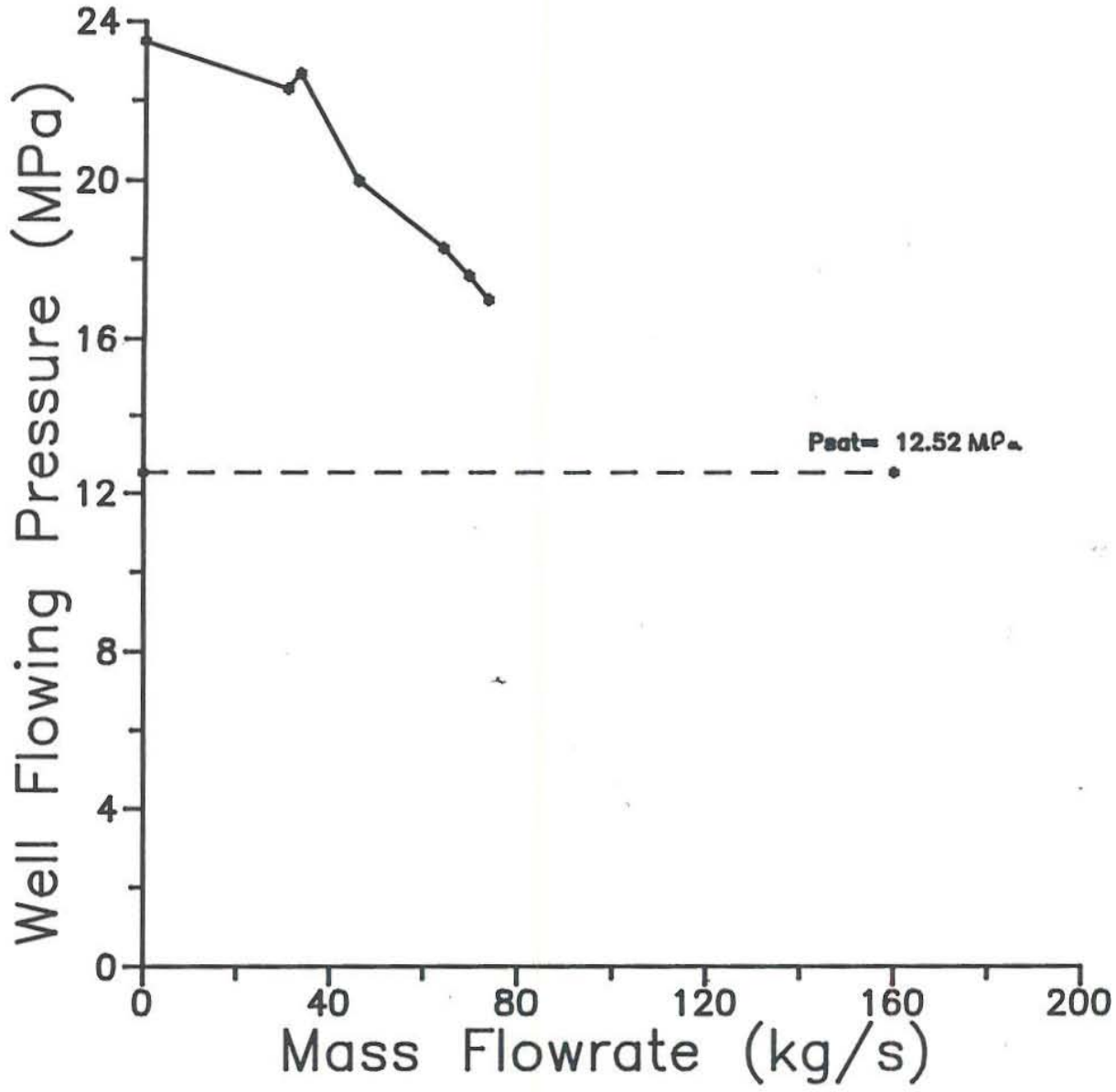

Figure 12- Inflow performance curve Well M-93 of Cerro Prieto.

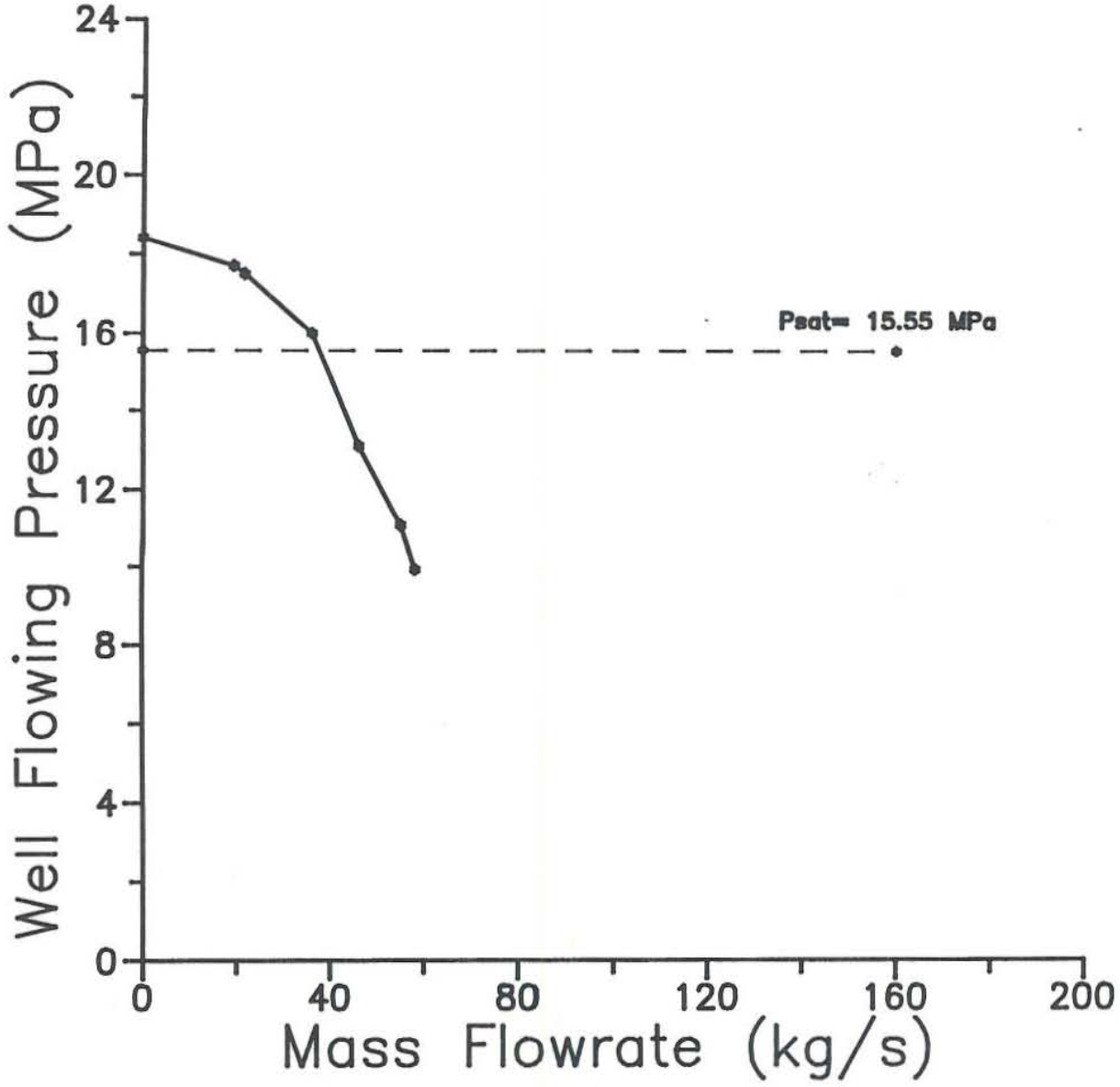

Figure 13- Inflow performance curve Well M-102 of Cerro Prieto.

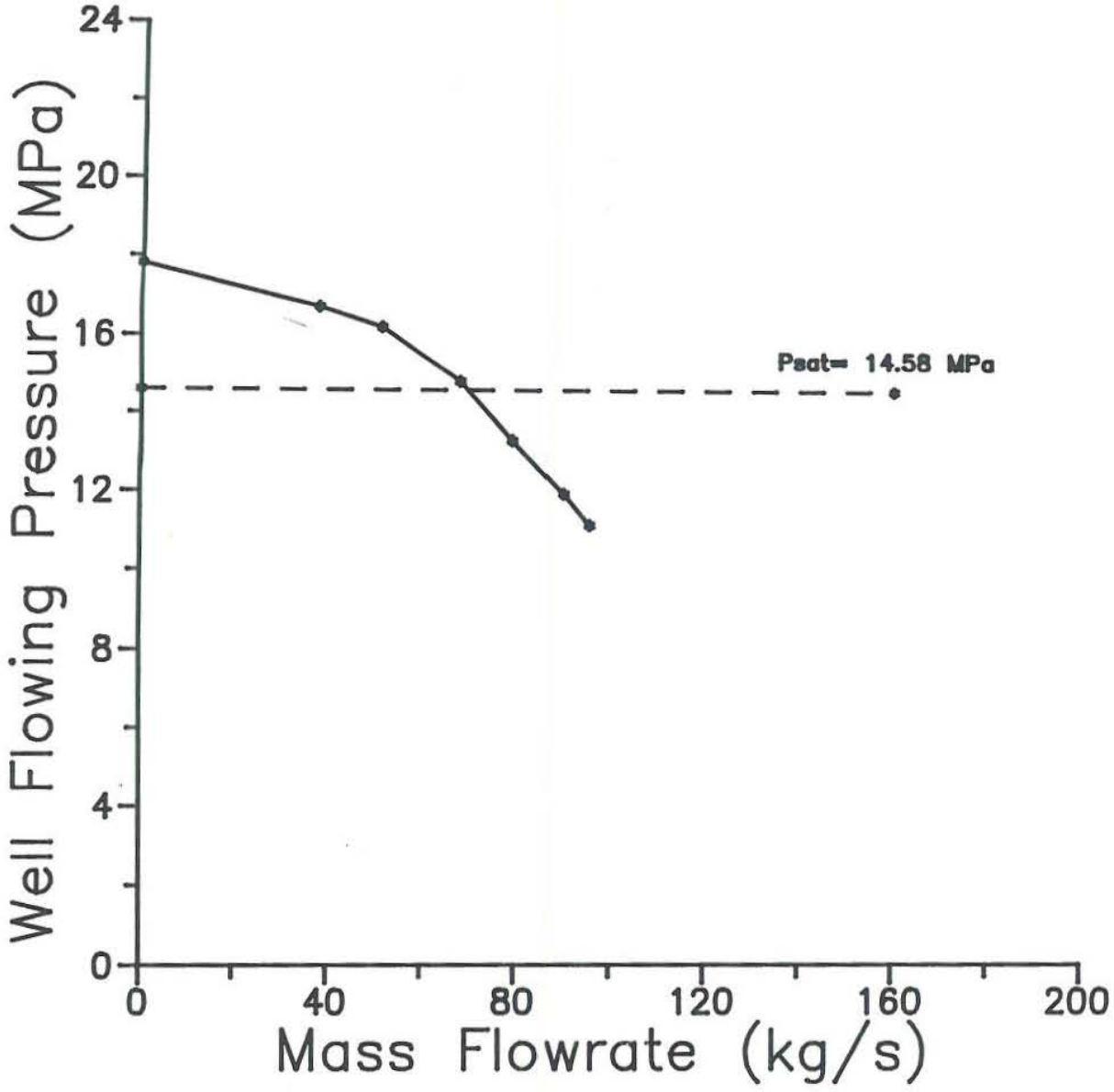

Figure 14- Inflow performance curve Well E-2 of Cerro Prieto.

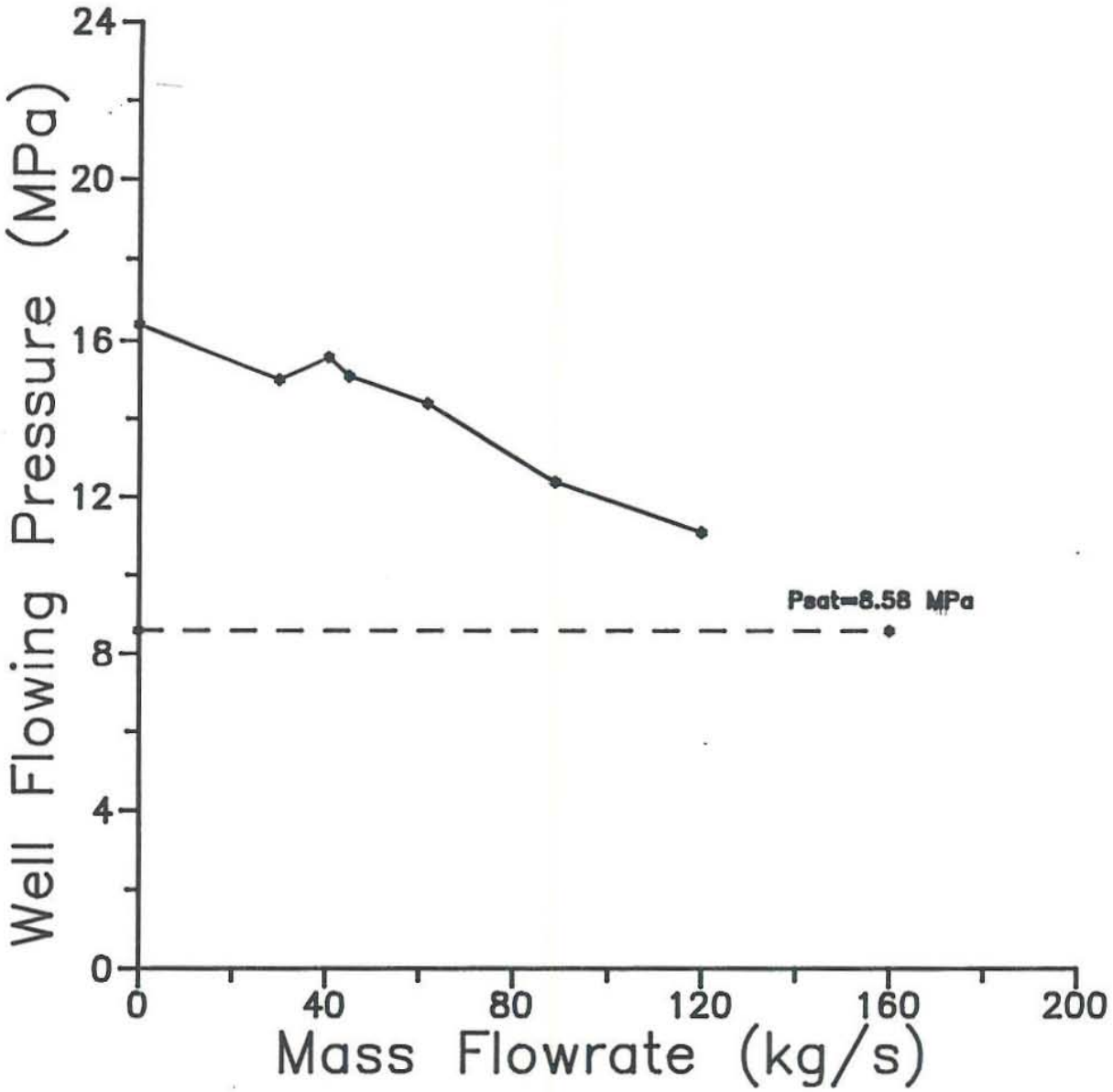

Figure 15- Inflow performance curve Well M-110 of Cerro Prieto.

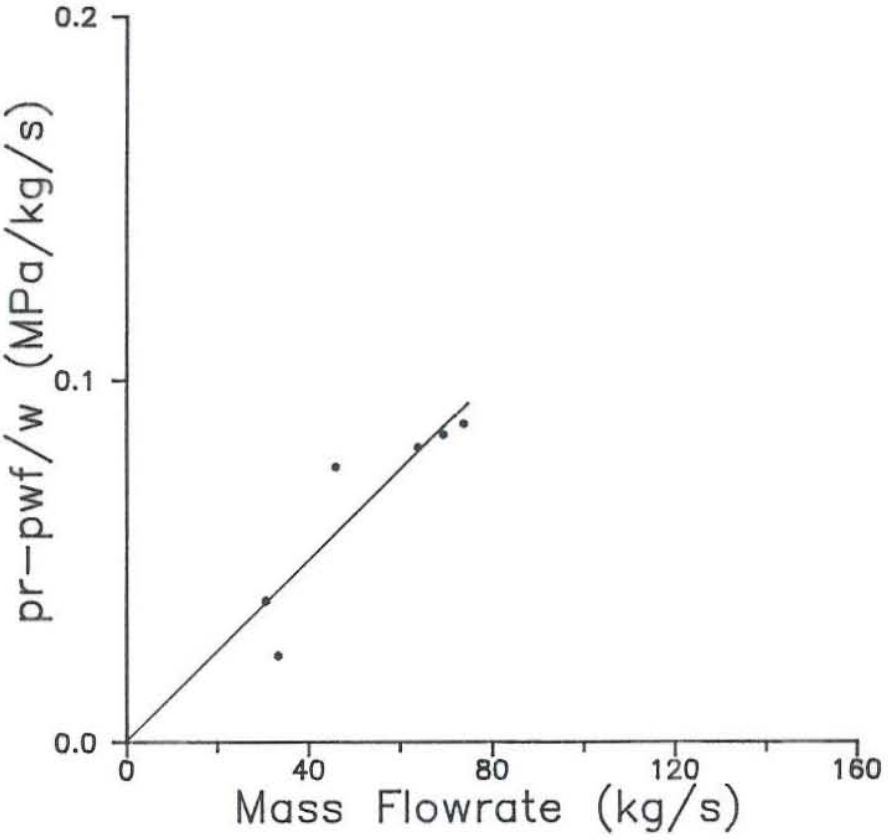

Figure 16- Turbulent effects present in data of Well M-93, the straight line through zero are shown.

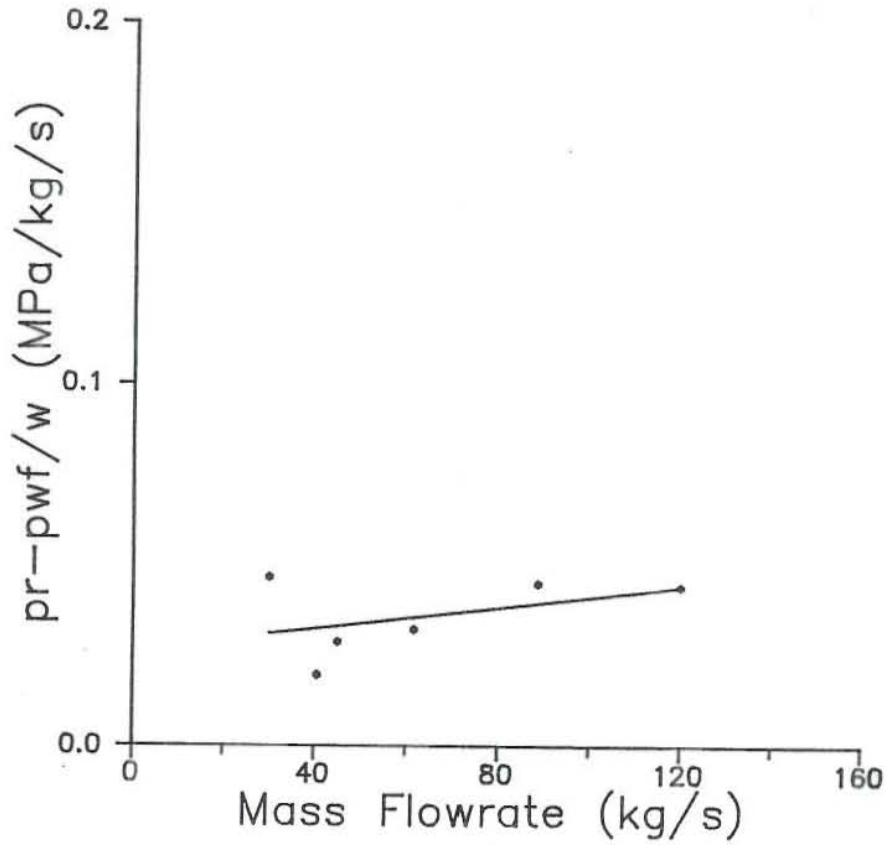

Figure 17- Turbulent and linear effects present in data of Well M-110.

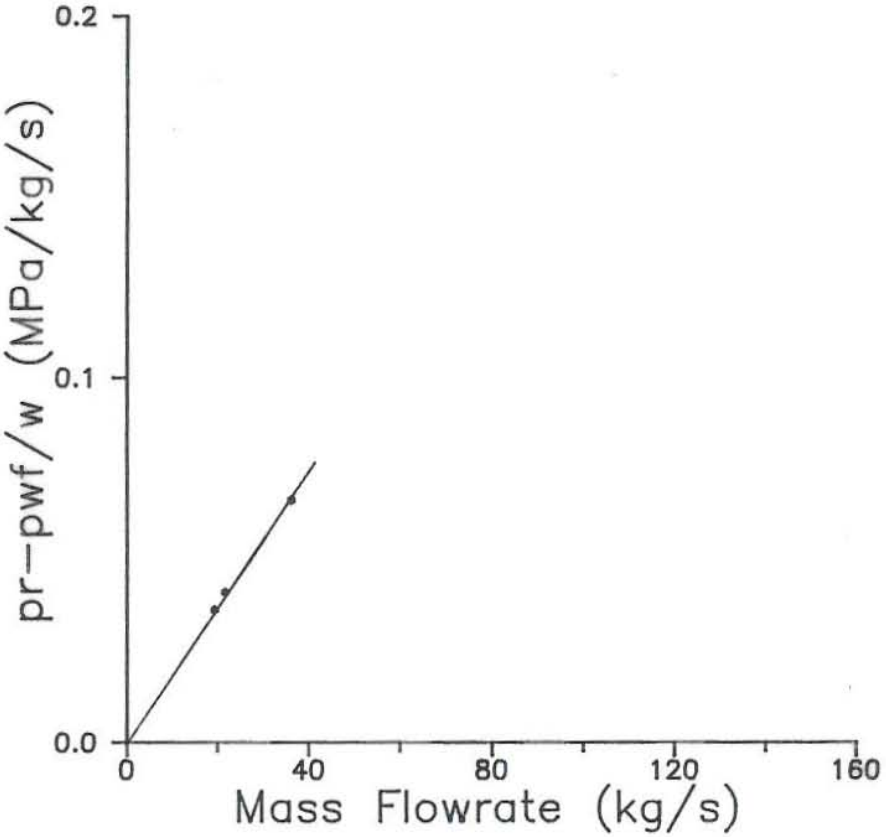

Figure 18- Turbulent effects in data of Well M-102 above saturation pressure, the straight line through zero are shown.

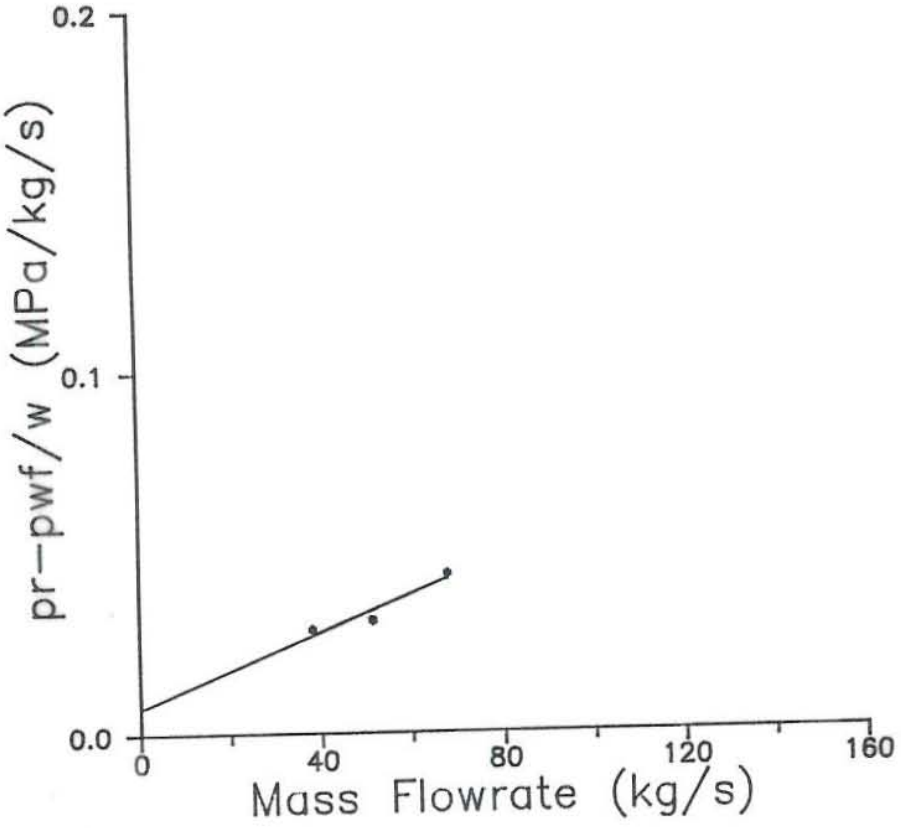

Figure 19- Turbulent effects in data of Well E-2 above saturation pressure, the straight line through zero are shown.

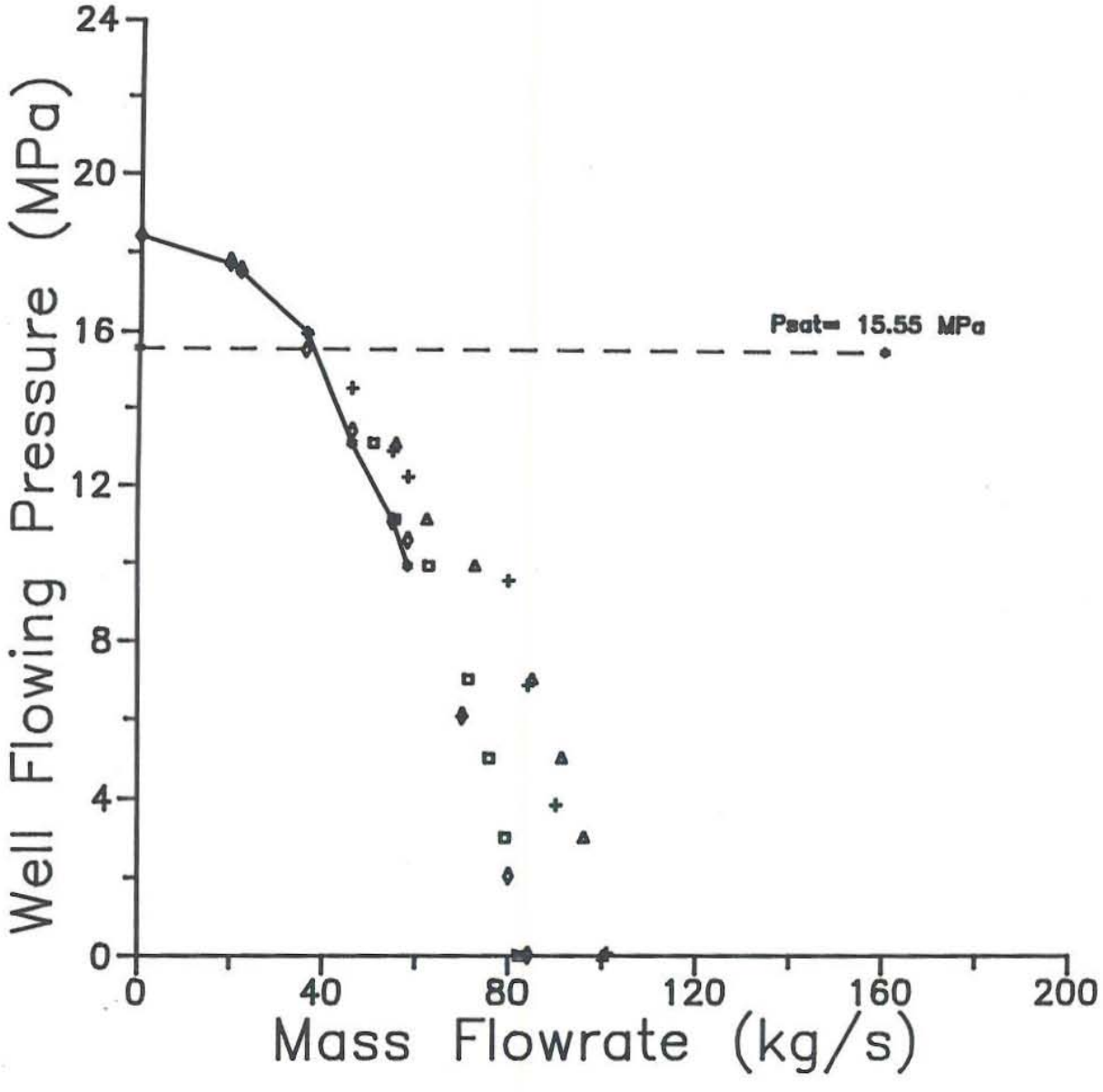

Figure 20- Different fits for Well M-102.

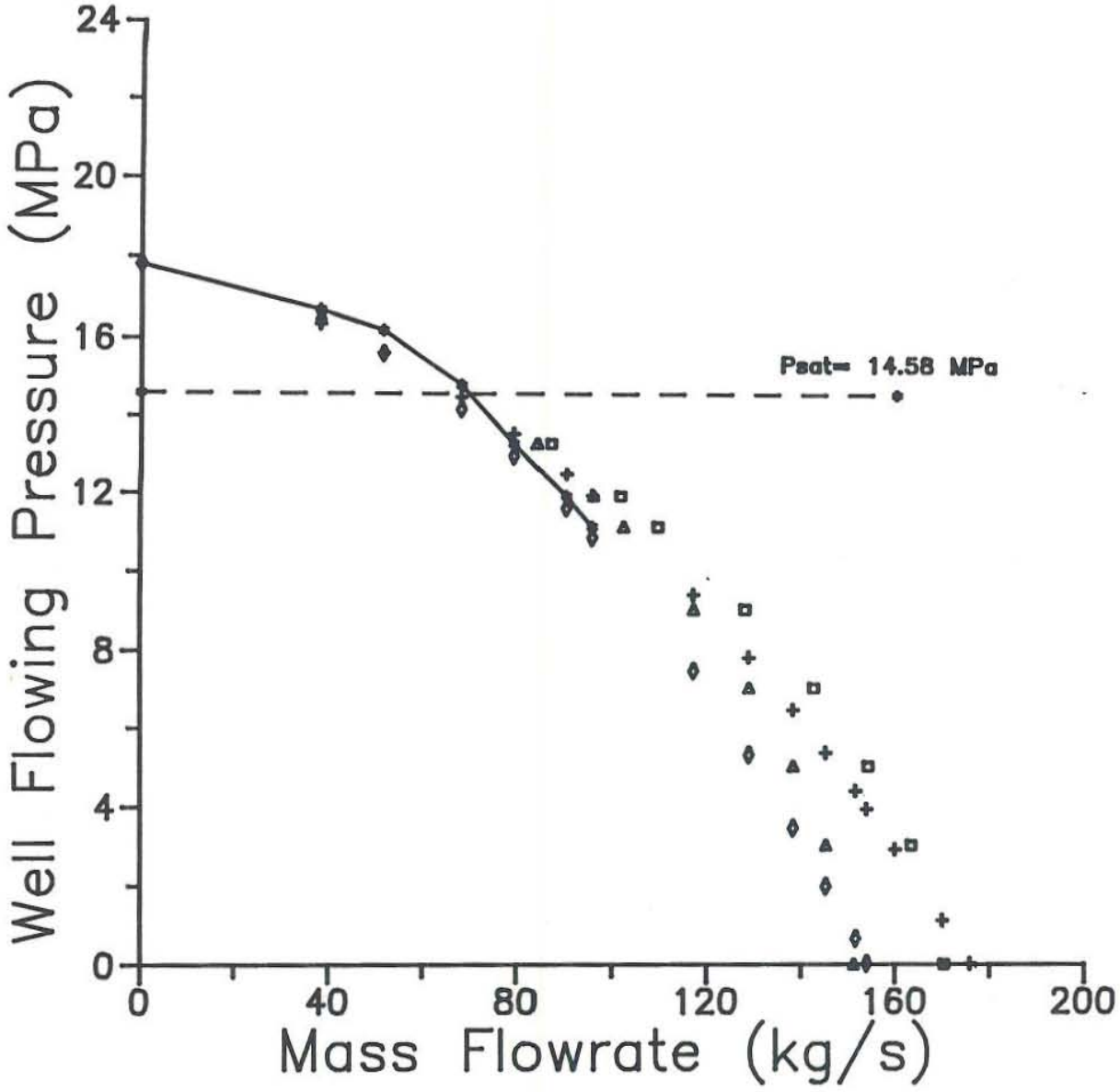

Figure 21- Different fits for Well E-2

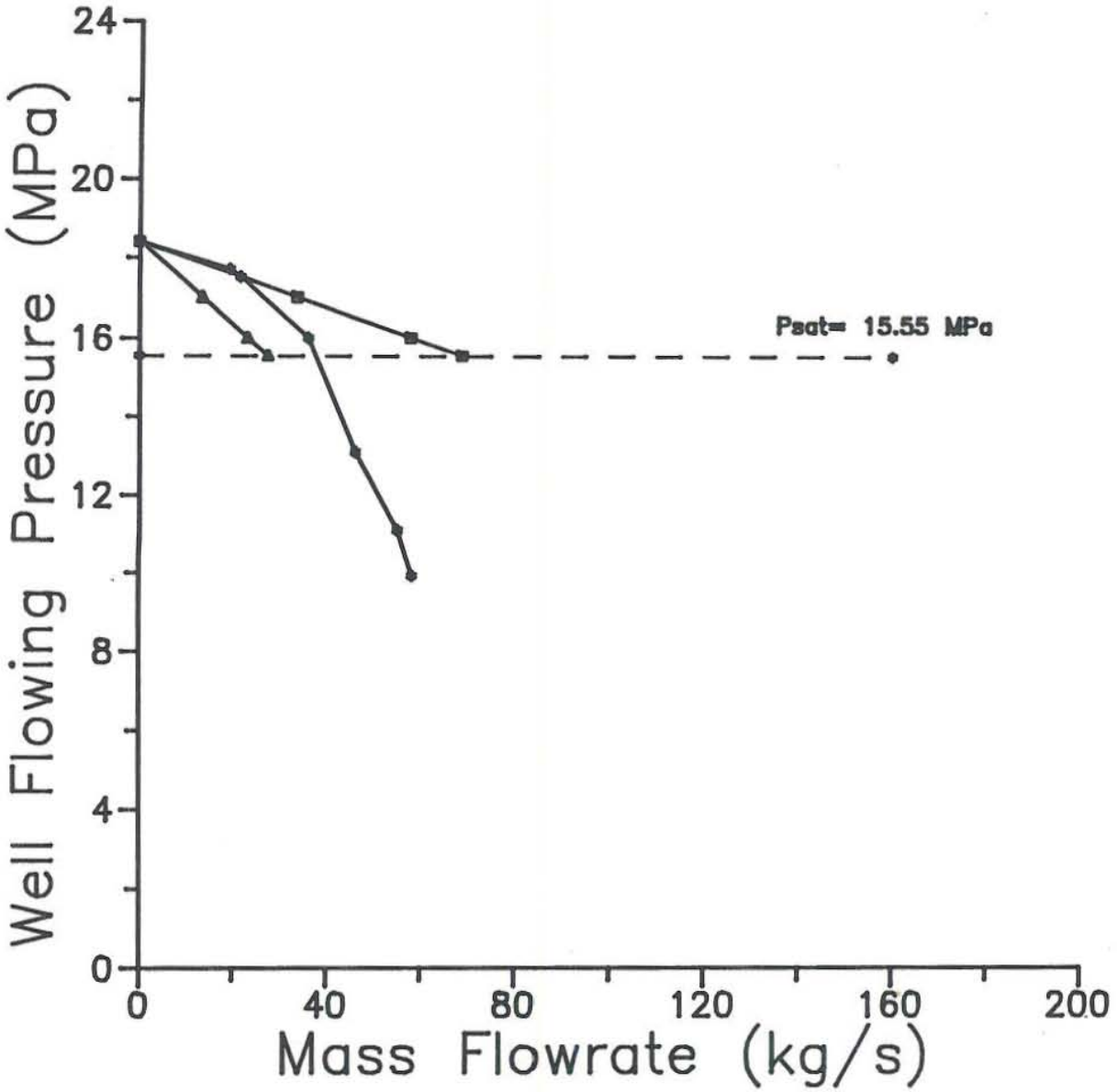

Figure 22- Comparatione of inflow performance curves Well M-102 of Cerro Prieto.

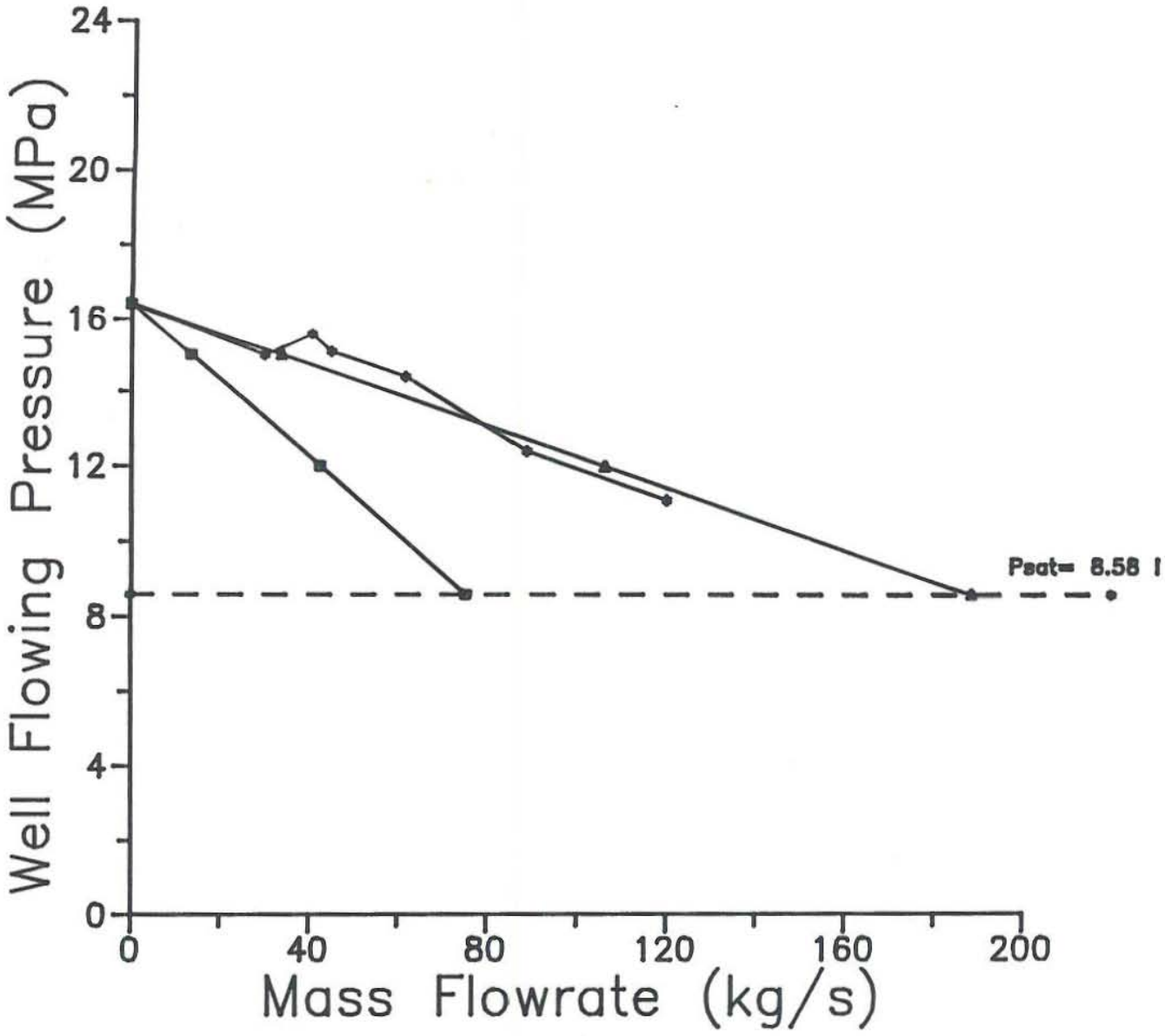

Figure 23- Comparatione of inflow performance curves Well E-2.

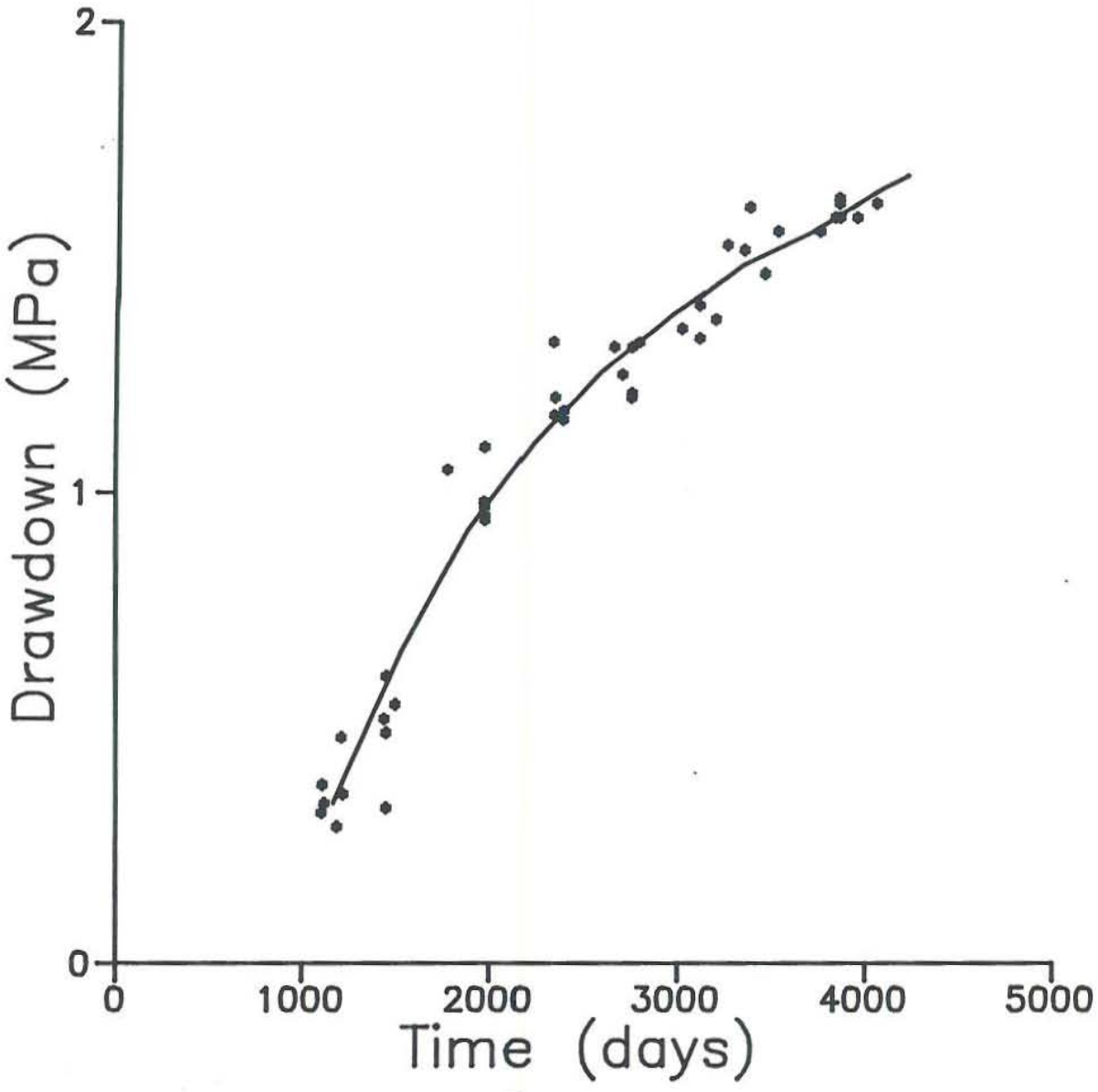

Figure 24- Drawdown of Svartsengi geothermal field.

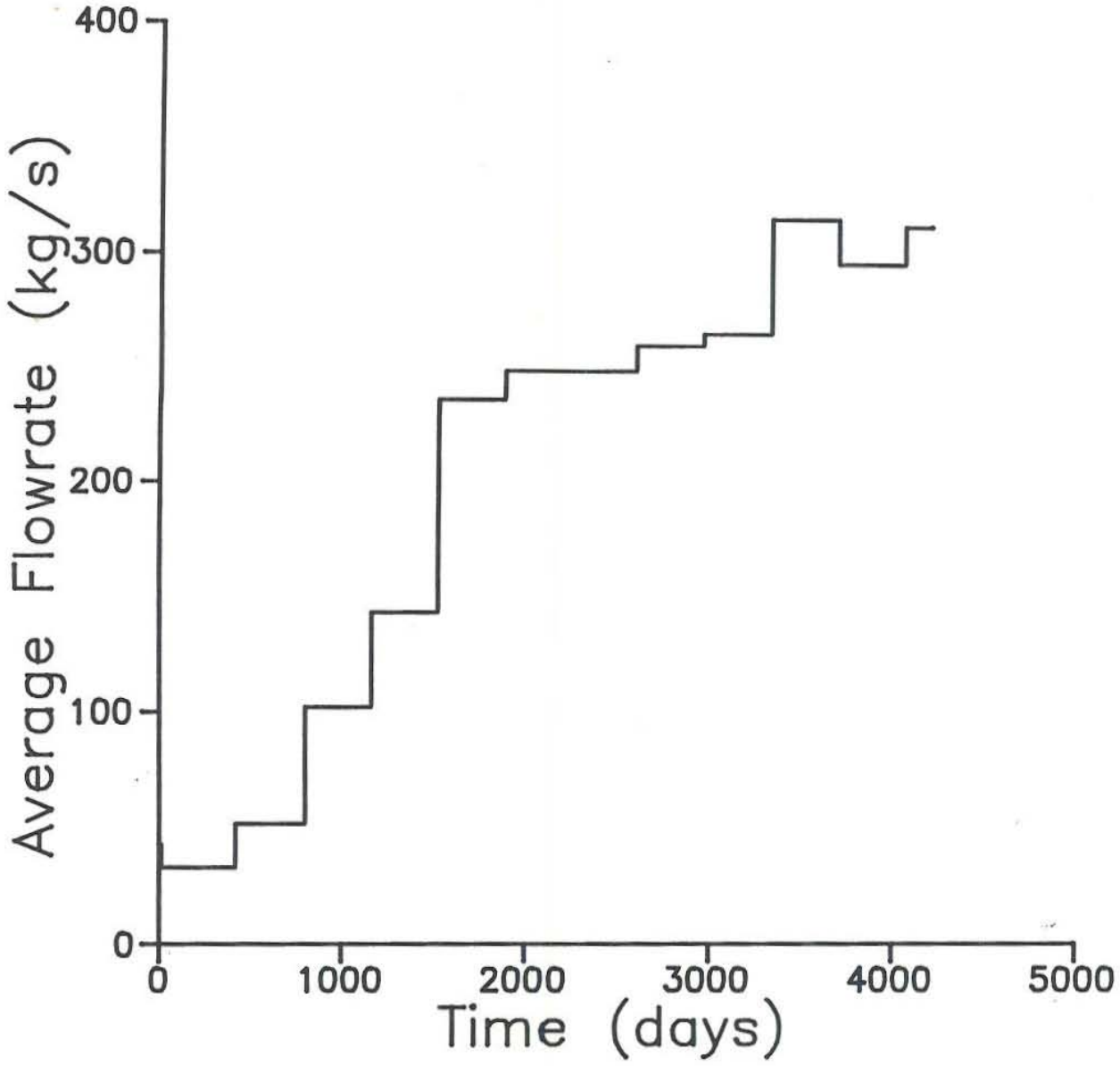

Figure 25- Average flowrate of Svartsengi geothermal field.

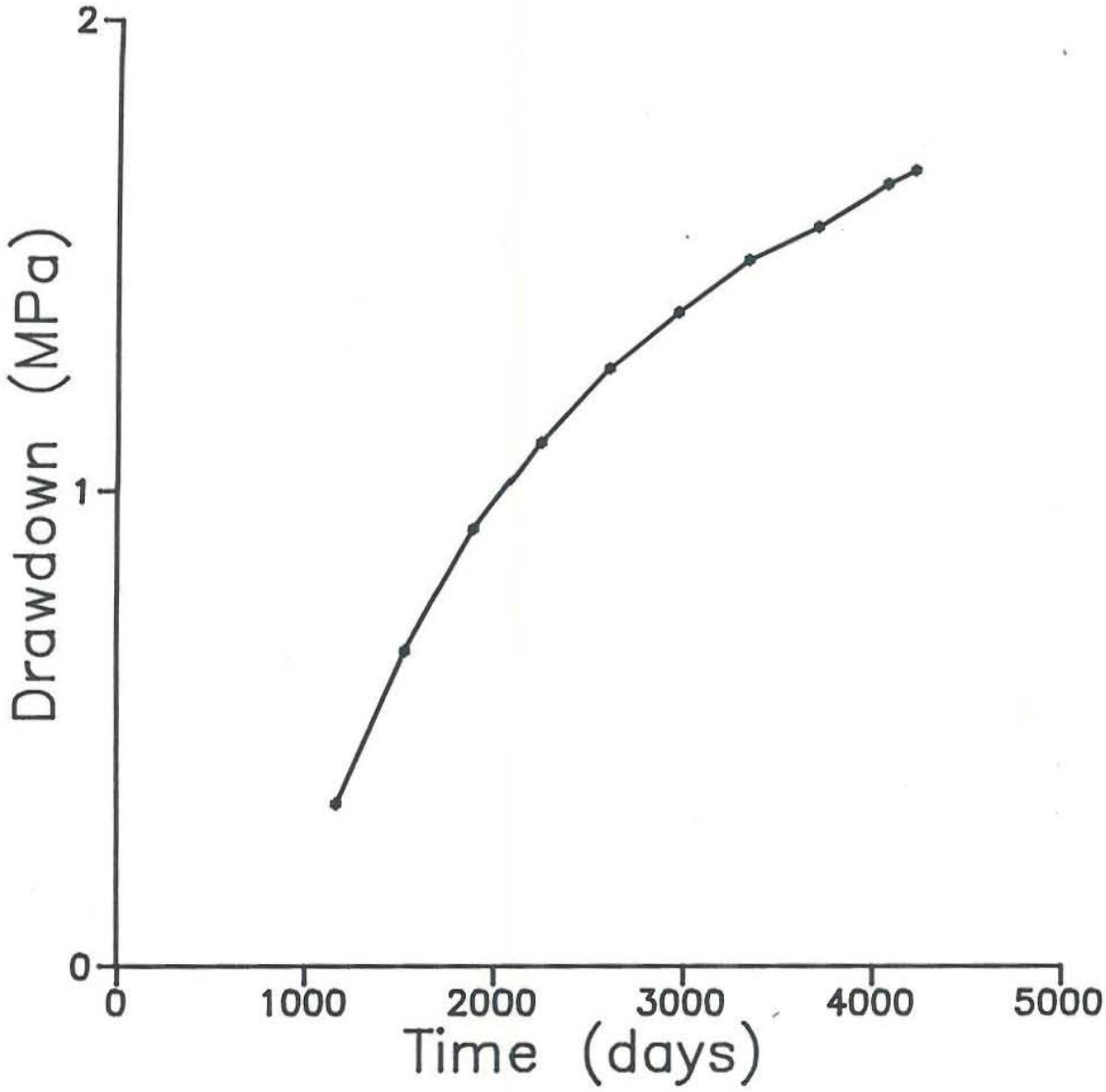

Figure 26- Drawdown fit of Svartsengi geothermal field.

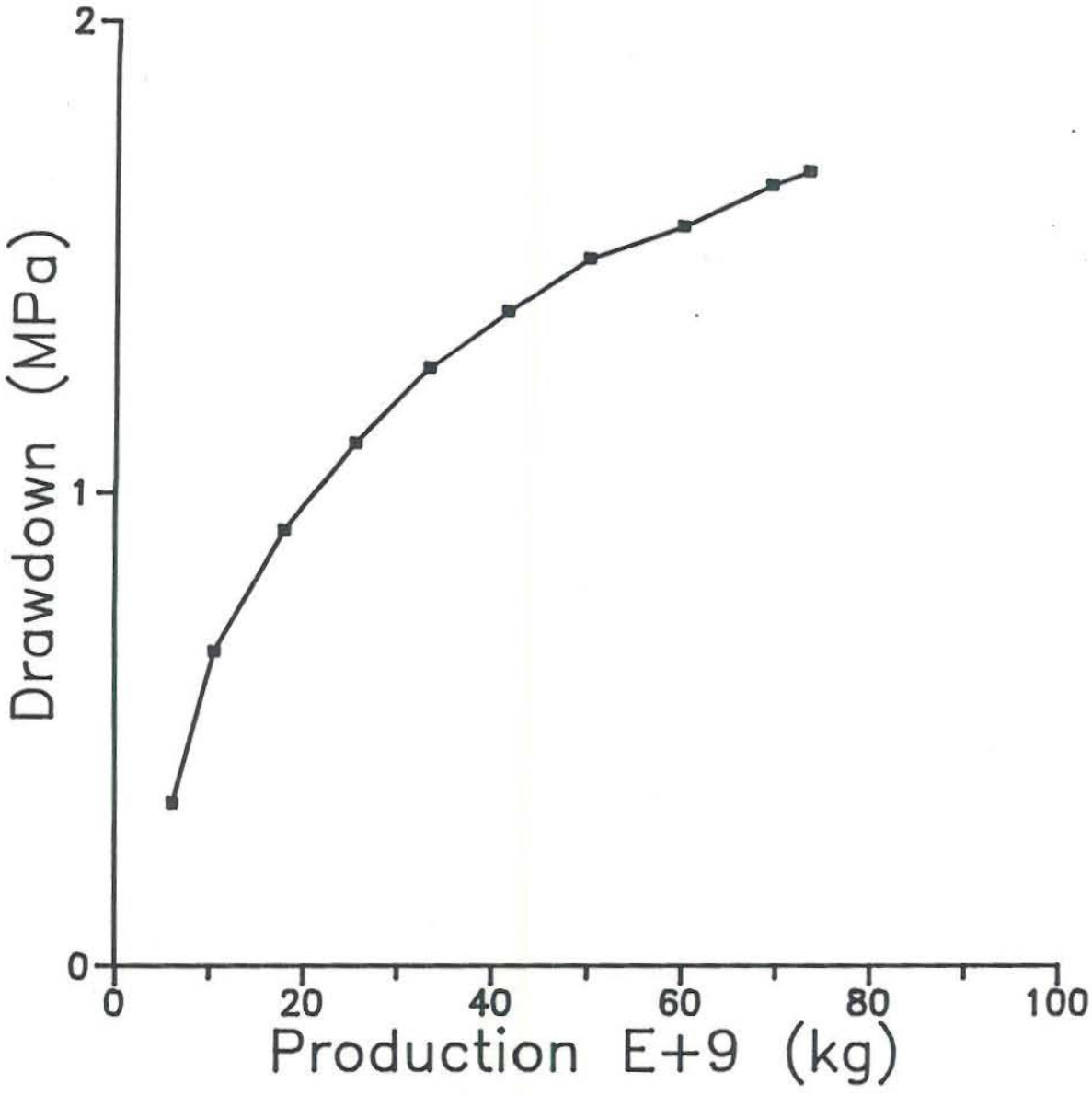

Figure 27- Accumulative mass production vs. drawdown of Svartsengi geothermal field.

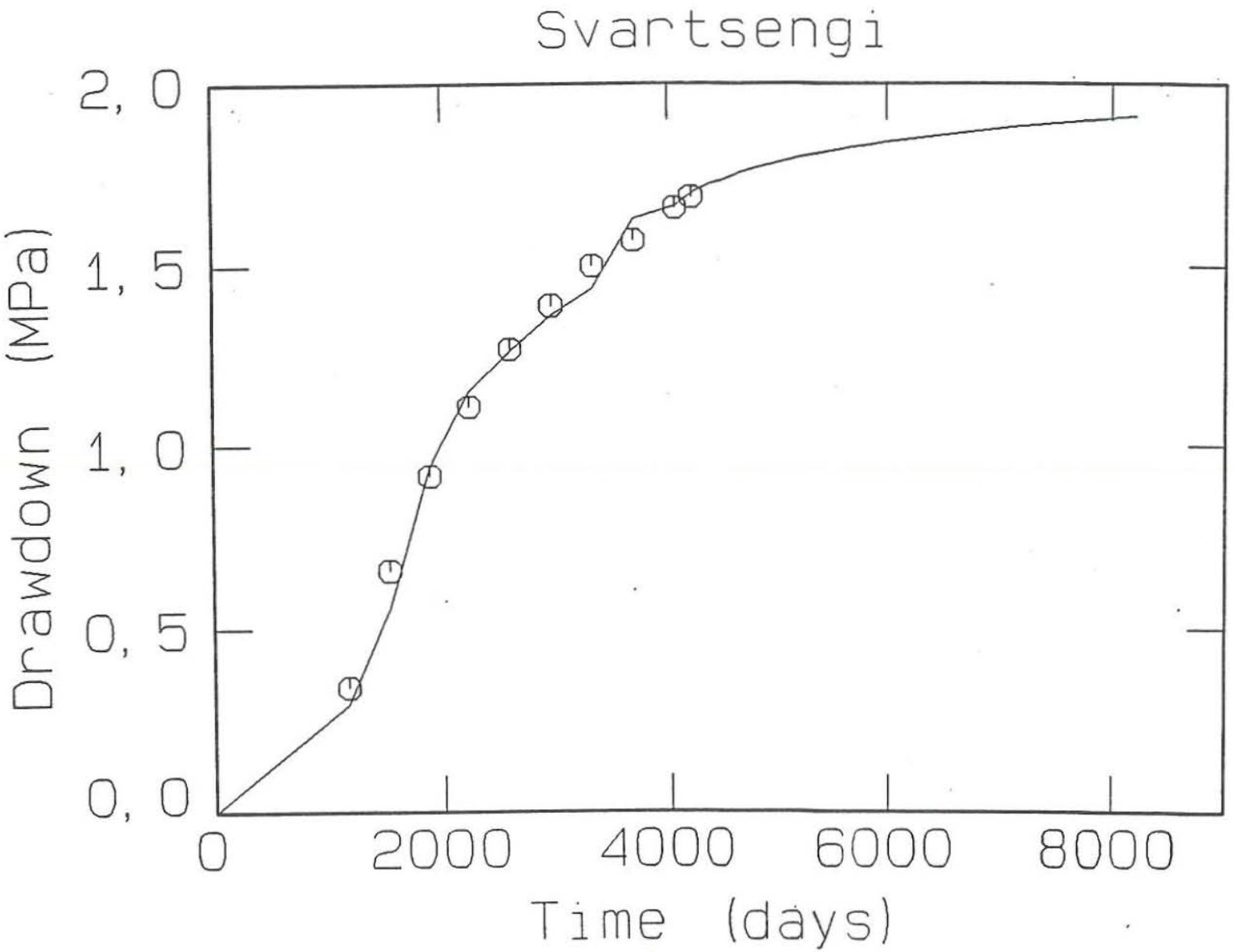

Figure 28- Radial Simplified Hurst model fit and forecast drawdown for Svartsengi geothermal field.

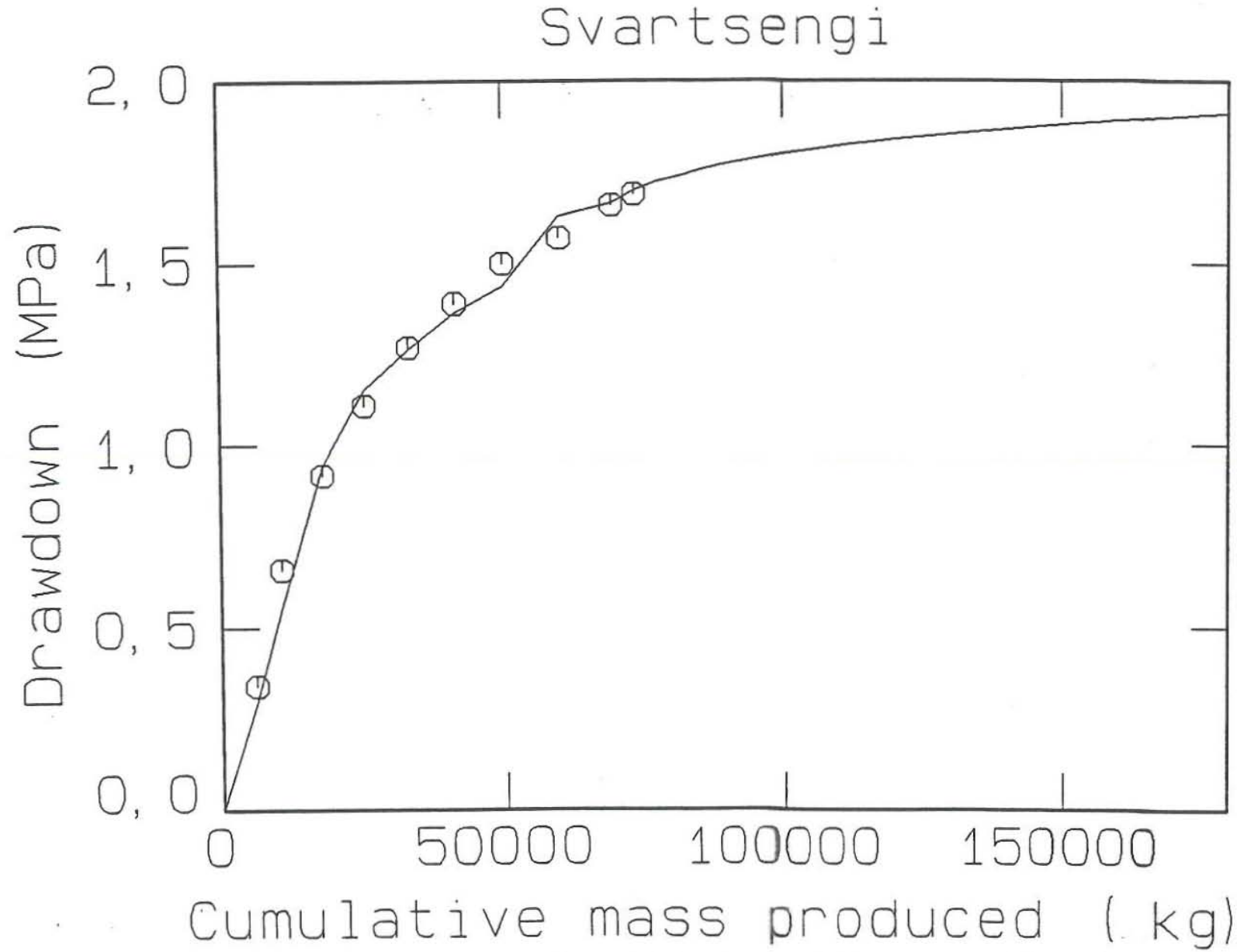

Figure 29- Radial Simplified Hurst model fit and forecast mass production for Svartsengi geothermal field.

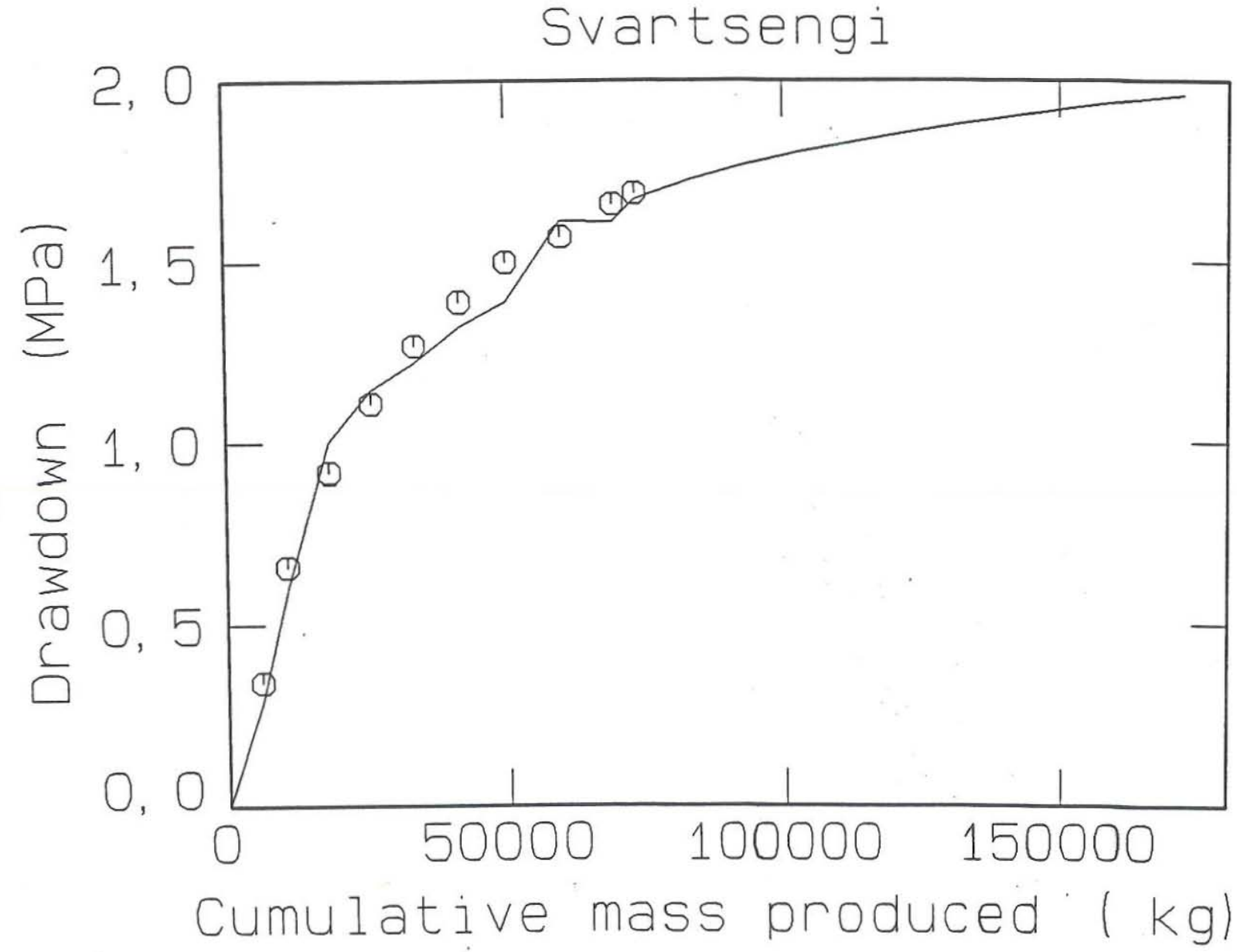

Figure 30- Line Source Solution model fit and forecast mass for Svartsengi geothermal field.

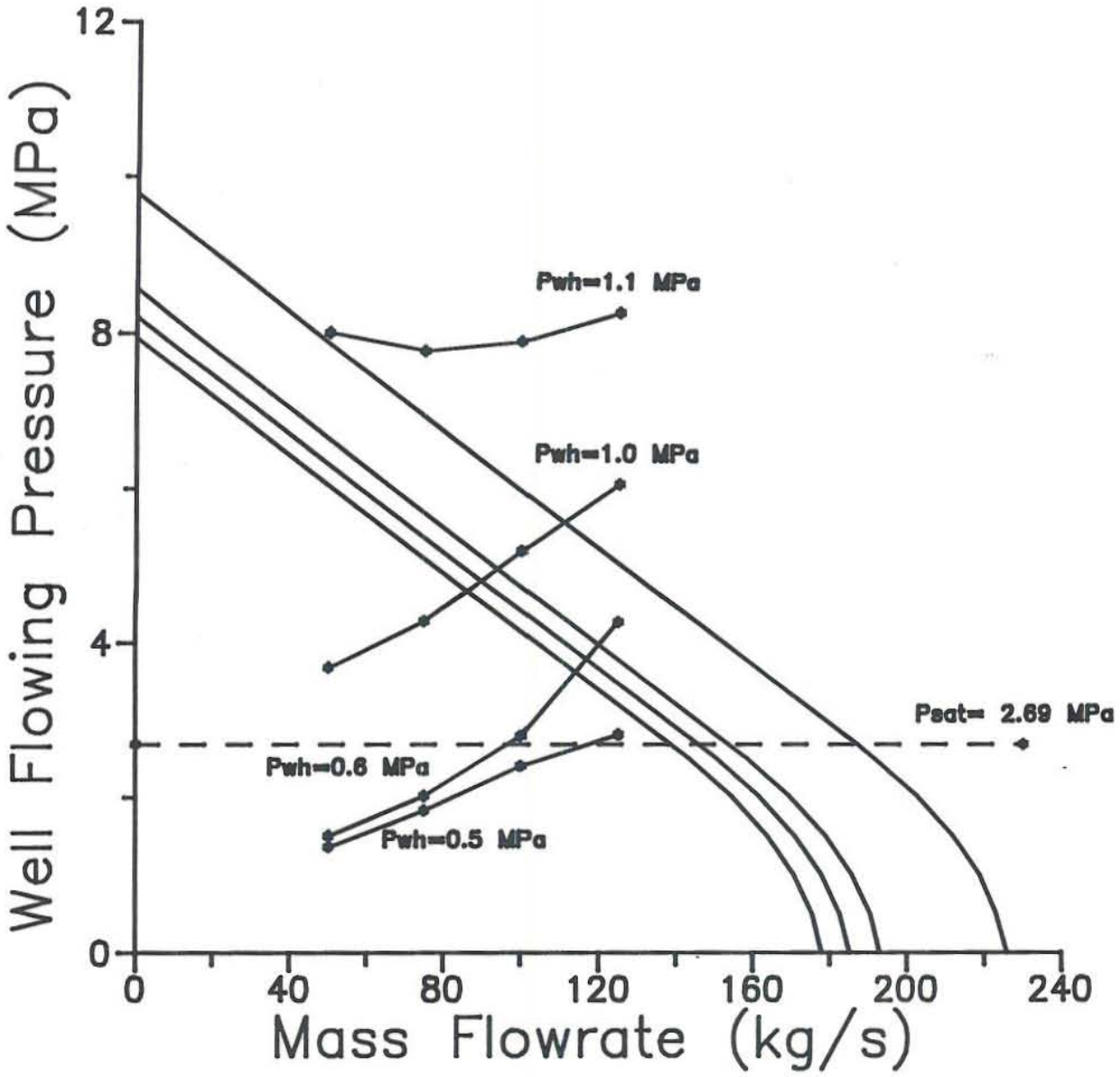

Figure 31- Deliverability of Well 12 of Svartsengi.

APPENDIX A

1

WELL SV-9

INPUT DATA AS FOLLOW:

WATER GRAVITY	1.0120
TOTAL MASS FLOWRATE,LB/HR	476295.5000
HEAT TRANSF COEFF,BTU/HR/SQ	.0000

AT THE WELLHEAD :

DEPTH,FT	.00
PRESSURE,PSIA	101.69
TEMPERATURE,F	328.99

PIPE DIAMETER USED AS FOLLOW:

FROM .0 FT TO 2952.0 FT, PIPE DIAMETER (FT) = 1.0344
ABS ROUGHNESS (FT) = .0003

TOTAL LENGTH DIVIDED IN 50 INTERVALS

DOWNHOLE SHUT-IN TEMPERATURE AS FOLLOW:

DEPTH,FT	TEMP,F
.00	77.00
2952.00	460.40

1

* TWO-PHASE FLOW * DEPTH FT.	PRES PSIA	TEMP F	ENTH BTU/LB	FRICTION Psi /100ft	ACCELE. Psi /100ft	POTENT. Psi /100ft	REGIME	qw/A ft/s	qs/A ft/s
.0	101.7	329.0	442.0						
59.0	103.9	330.5	442.0	2.669	.000	.991	SLUG	2.32	108.00
118.1	106.0	332.0	442.0	2.594	.000	1.020	SLUG	2.32	104.90
177.1	108.1	333.4	442.0	2.523	.000	1.049	SLUG	2.33	101.92
236.2	110.2	334.8	442.0	2.455	.000	1.078	SLUG	2.33	99.11
295.2	112.2	336.2	442.0	2.393	.000	1.106	SLUG	2.34	96.51
354.2	114.3	337.6	442.0	2.332	.000	1.135	SLUG	2.35	93.99
413.3	116.3	338.9	442.0	2.275	.000	1.163	SLUG	2.35	91.64
472.3	118.3	340.2	442.0	2.218	.000	1.193	SLUG	2.36	89.28
531.4	120.3	341.4	442.0	2.164	.000	1.223	SLUG	2.36	87.02
590.4	122.3	342.6	442.0	2.113	.000	1.253	SLUG	2.37	84.91
649.4	124.3	343.9	442.0	2.064	.000	1.283	SLUG	2.37	82.84
708.5	126.3	345.0	442.0	2.016	.000	1.314	SLUG	2.38	80.85
767.5	128.2	346.2	442.0	1.971	.000	1.344	SLUG	2.38	78.99
826.6	130.2	347.4	442.0	1.927	.000	1.375	SLUG	2.39	77.15
885.6	132.1	348.5	442.0	1.885	.000	1.405	SLUG	2.39	75.43
944.6	134.0	349.6	442.0	1.844	.000	1.436	SLUG	2.40	73.72
1003.7	136.0	350.7	442.0	1.804	.000	1.468	SLUG	2.40	72.08
1062.7	137.9	351.8	442.0	1.767	.000	1.499	SLUG	2.41	70.53
1121.8	139.8	352.9	442.0	1.730	.000	1.531	SLUG	2.41	69.00
1180.8	141.8	353.9	442.0	1.695	.000	1.563	SLUG	2.42	67.52
1239.8	143.7	355.0	442.0	1.661	.000	1.595	SLUG	2.42	66.13

1476.0	151.4	359.1	442.0	1.532	.000	1.730	SLUG	2.44	60.76
1535.0	153.3	360.1	442.0	1.502	.000	1.764	SLUG	2.45	59.52
1594.1	155.2	361.1	442.0	1.473	.000	1.800	SLUG	2.45	58.28
1653.1	157.2	362.1	442.0	1.444	.000	1.836	SLUG	2.46	57.11
1712.2	159.1	363.0	442.0	1.416	.000	1.872	SLUG	2.46	55.93
1771.2	161.1	364.0	442.0	1.388	.000	1.910	SLUG	2.47	54.78
1830.2	163.0	365.0	442.0	1.362	.000	1.947	SLUG	2.47	53.69
1889.3	165.0	366.0	442.0	1.336	.000	1.985	SLUG	2.47	52.59
1948.3	166.9	366.9	442.0	1.311	.000	2.023	SLUG	2.48	51.56
2007.4	168.9	367.8	442.0	1.286	.000	2.063	SLUG	2.48	50.51
2066.4	170.9	368.8	442.0	1.261	.000	2.104	SLUG	2.49	49.49
2125.4	172.9	369.7	442.0	1.238	.000	2.143	SLUG	2.49	48.52
2184.5	174.9	370.7	442.0	1.214	.000	2.185	SLUG	2.50	47.54
2243.5	176.9	371.6	442.0	1.192	.000	2.226	SLUG	2.50	46.61
2302.6	179.0	372.5	442.0	1.169	.000	2.269	SLUG	2.51	45.68
2361.6	181.0	373.5	442.0	1.147	.000	2.313	SLUG	2.51	44.76
2420.6	183.1	374.4	442.0	1.126	.000	2.356	SLUG	2.52	43.89
2479.7	185.1	375.3	442.0	1.105	.000	2.402	SLUG	2.52	42.99
2538.7	187.2	376.2	442.0	1.084	.000	2.448	SLUG	2.52	42.13
2597.8	189.3	377.2	442.0	1.063	.000	2.497	SLUG	2.53	41.26
2656.8	191.4	378.1	442.0	1.043	.000	2.545	SLUG	2.53	40.43
2715.8	193.6	379.0	442.0	1.023	.000	2.595	SLUG	2.54	39.59
2774.9	195.7	379.9	442.0	1.003	.000	2.647	SLUG	2.54	38.76
2833.9	197.9	380.9	442.0	.984	.000	2.698	SLUG	2.55	37.97
2893.0	200.1	381.8	442.0	.965	.000	2.752	SLUG	2.55	37.17
2952.0	202.3	382.7	442.0	.947	.000	2.806	SLUG	2.56	36.41

**** PRESSURE ANALYSIS ****

TOTAL FRICTION, LIQUID	=	.0000 PSI
TOTAL POTENTIAL, LIQUID	=	.0000 PSI
TOTAL FRICTION, TWO-PHASE	=	47.5295 PSI
TOTAL POTENTIAL, TWO-PHASE	=	53.0896 PSI
TOTAL ACCELE., TWO-PHASE	=	.0000 PSI

APPENDIX B

APPENDIX B

Equation 4 can be written

$$\frac{\Delta w}{\Delta w_{max}} = 1.0 - \frac{0.2}{p_{sat}} p_{wf} - \frac{0.8}{(p_{sat})^2} p_{wf}^2 \qquad \text{(i)}$$

Introducing constant

$\Delta w_{max} = k_1$, $0.2/p_{sat} = k_2$ and $0.8/(p_{sat})^2 = k_3$

the equation (i) take the form

$$\Delta w/k_1 = 1.0 - k_2\, p_{wf} - k_3\, pw_f^2 \qquad \text{(ii)}$$

if derivative is taking

$$dw/k_1 = - k_2\, dpw_f - 2k3\, p_{wf}\, dp_{wf} \qquad \text{(iii)}$$

divided all the equation by dw

$$1/k_1 = - k_2\, dp_wf/dw - 2k_3\, p_{wf}\, dp_{wf}/dw \qquad \text{(iv)}$$

take common factor

$$1/k_1 = - (k_2 + 2k_3\, p_{wf})\, dp_{wf}/dw \qquad \text{(v)}$$

if $p_{wf} = p$ and $dp_{wf}/dw = dp/dw$

therefore

$$1/k_1 = - (k_2 + 2k_3\, p)\, dp/dw \qquad \text{(vi)}$$

if in the equation (vi) is substituted the k's values to find Δw_{max}.

$$1/\Delta w_{max} = - (0.2/p_{sat} + 2 (0.8/p_{sat})^2\, p)\, dp/dw \qquad \text{(vii)}$$

if the operation is done in the equation vii

$$1/\Delta w_{ax} = - (0.2/p_{sat} + 0.8/p_{sat})\, dp/dw \qquad \text{(viii)}$$

$$1/\Delta w_{max} = - (1.8/p_{sat})\, dp/dw \qquad \text{(ix)}$$

the equation ix can be write in different forms

$$\Delta w_{max} = -(p_{sat}/1.8)\, dw/dp = P_{sat}\, J/1.8 \qquad \text{(x)}$$

Equation ix is the same as equation 3 .